UNIVERSITÀ DELLA CALABRIA

UNIVERSITA' DELLA CALABRIA

Dipartimento di Informatica Modellistica Elettronica e Sistemistica

Dottorato di Ricerca in

Ingegneria dei Sistemi ed Informatica

CICLO

XXVII

Software Defined System for Radar Development and Applications

Settore Scientifico Disciplinare ING/INF 02

Coordinatore: Ch.mo Prof. Sergio GRECO

Firma 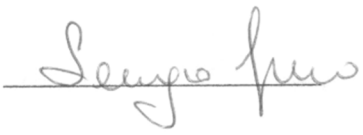

Supervisore/Tutor: Ch.mo Prof. Giuseppe DI MASSA

Firma 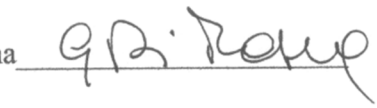

Supervisore/Tutor: Ch.ma Prof.ssa Sandra COSTANZO

Firma 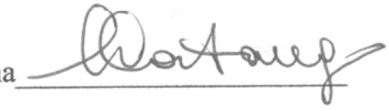

Dottorando: Dott. Francesco SPADAFORA

Firma 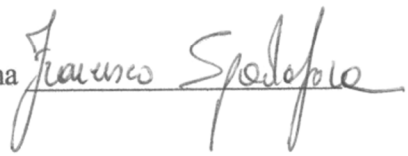

to my wife, for her love

Introduzione

Negli ultimi anni le nuove tecnologie relative ai sistemi radar hanno attirato l'attenzione di molti ricercatori e scienziati. In un'ottica di efficienza, i nuovi sistemi di comunicazione e misura sono orientati al software al fine di eliminare completamente i limiti imposti dalle architetture hardware. L'idea di sostituire i componenti hardware, come mixer, filtri ecc. con componenti software, ha segnato una nuova forntiera nel mondo della ricerca, specialmente nelle comunicazioni wireless. I sistemi Softare Defined Radio hanno rivoluzionato totalmente il mondo dell'Information and Communication Technology. Successivamente, tale concetto si è diffuso in diverse aree di ricerca fornendo eccellenti risultati nel campo dei sistemi radar. Questo scritto tratta principalmente le potenzialità dei sistemi Software Defined Radar (**SDRadar**); inoltre, il lavoro è principalmente focalizzato sullo sviluppo sviluppo di un sistema SDRadar adatto al monitoraggio frane.

Nel primo capitolo vengono descritte le potenzialità della piattaforma USRP (Universal Software Radio Peripheral); in particolare viene dimostrato come questa piattaforma, ideata per applicazioni relative alla didattica sui sistemi wireless, sia adattabile ad applicazioni di tipo radar, offrendo una buona soluzione sia in termini di performance che di costi di produzione.

L'architettura sia hardware che software del sistema SDRadar sviluppato viene trattata nella seconda parte del primo capitolo, mentre la terza parte include la validazione sperimentale dell'intero sistema attraverso i test in camera anecoica ed in campo aperto.

Nel secondo capitolo invece, viene presentato un algoritmo innovativo per il rilevamento delle caratteristiche elettriche del suolo basato sull'uso di segnali OFDM. In fine, nel capitolo 3 viene discusso lo stato dell'arte di tali sistemi includendo una breve introduzione sui sistemi radar di prossima generazione.

Acknowledgements

The accomplishments in this work were made possible by the help and support of many people.
First, and foremost, I would like to express my sincere gratitude to my supervisors, Prof.ssa Sandra Costanzo and Prof Giuseppe Di Massa, for their continuous guidance, suggestions, patience, and friendship during the course of my PhD. They have contributed tremendously to the scientific content of this dissertation. I am very fortunate to know Antonio Costanzo, he is a continuous resource for me , a great and old friend but also a big *man of science*; our friendship will never end.
I would especially like to thank Antonio Borgia; I will always remember his goodness towards me and his suggestions; I am happy to meet him.

Finally, I would like to thank my wife Angela and my parents, for their constant support, motivation and love, which allowed me to carry out, in the best way, this research programme.

Preface

In recent years, several emerging technologies in modern radar system design are attracting the attention of radar researchers and scientists. In the efficiency point view, the new communication and measurement systems are *software oriented* in order to completely avoid the limits and the costs due to the hardware architecture.
The idea to replace all the hardware components, like mixers, filters etc., with software components with the same task marked a new research frontier especially in wireless communication. Pioneers of the this step are the Software Defined Radio System that have totally revolutionized the world of information and communication technologies. Subsequently, this concept has spread in several areas of research providing great results in radar field
This thesis deals mainly with the potentialities of the Software Defined Radar system **(SDRadar)**; the work is especially focused on the development of a SDRadar system for the landslide monitoring.

In the first chapter the potentialities of the board USRP (Universal Software Radio Peripheral) are described, in particular it is shown how this platform, born for didactic application on wireless systems, is very suitable for radar application, providing a good solution in terms of performance and costs. The hardware and software architecture description of the developed SDRadar system is discussed in the second part of the first chapter while, the third part deals with the experimental validation of the entire system through anechoic chamber and open space tests.

The second chapter treats an application of a Software Defined Measurement system. A novel algorithm, based on the new OFDM radar signal pro-

cessing, for the soil electrical properties detection is presented. Finally ,in chapter 3, a complete state of art of these technologies, providing a detailed attention on the future radar, is presented.

Rende (CS) Italy, *Francesco Spadafora*
November 2014

Contents

List of Figures

List of Tables

1

L-band Software Defined Radar

1.1 Software Defined Radar

Software Defined systems have revolutionized the classical world of information and communication technologies providing great space for research in different areas. This modern idea takes place first in radio communication with Software Defined Radio (SDR) and subsequently, in many other fields like Software Defined Networking (SDN), Software Defined Measurement system (SDM), Software Defined Storage (SDS) and also in radar field with the Software Defined Radar System (SDRadar). The Software Defined Radar concept is based on the same principle as that of Software Defined Radio or rather, the components that in a classical radio or radar systems are implemented using dedicated hardware (mixer, filter, modulator, etc.) in a Software Defined System they are implemented via software. The main idea is the directly digitalization of the signal after the antenna situated in reception and the directly digital to analogue conversion before the antenna situated in transmission; figure 1.1 shows the ideal configuration of a SDRadar system. The flexibility of software based systems and their easy adaptability make them useful for many different applications, as shown in radar context. Since the radar platform is completely software defined, it can easily switch between different operations mode by simply modifying both the transmitted waveforms and the signal processing tasks on the fly. The main benefits are in the possibilities to create multipurpose radar with the same hardware and in the easy implementation of new signal processing techniques; but, above all, the systems homogeneity and standardization with a dramatically reduction of costs [1]. In practical realization of the system in figure 1.1 the main problems are in the digital to

analogue converter (DAC) and in analogue to digital converter (ADC). The high operation frequency of a generically radar system imposes the ADC sampling rate, for Shannon/Nyquists theorems, at least the double of the antenna frequency in order to have a correctly conversion. ADC and DAC converters, able to work at high frequency, are not for sale or are expensive. Figure 1.2 shows the state of art of the ADC converter [1]. To solve this problem two fundamental blocks have been added in the ideal block diagram (figure 1.3), a Radio Frequency Front End (RF-front-end) and a Field Programmable Gate Array (FPGA). The RF front-end is the only analogue block in a software defined radar system. In receiver path, this block shifts the signal frequency received from the antenna to an intermediate frequency or in baseband; while, in transmitter path the RF front-end shifts the signal from baseband frequency to a desired carrier frequency. This operation is necessary in order to have a correct A/D conversion. The Field Programmable Gate Array (FPGA) is a programmable integrated circuit; it is generally used for signal processing operations with digital data. The main task is a pre-elaboration of the radar data and the adaptation of the data-flow to the interface of Pc connection. In radar application, where a strong data elaboration is required, an adequate elaboration speed and hardware interface with high throughput are necessary. In particular, the bandwidth of the interface is related to the radar range resolution and presents a strong limitation [2]. Debatty in the paper Software Defined Radar the State of Art was one of the first to analyse this problem and compare and contrast several kinds of hardware interfaces. In table 2.1 a list of the most popular hardware interfaces of connection are compared [3].

Many scientists and researchers are focusing their attention on SDRadar systems and many testbed and applications have been developed by considering the Universal Software Radio Peripheral (USRP) motherboard [4] as hardware base, and GNU Radio, an open source software defined radio project, as a software tool to implement very sophisticated, low cost SDRadar applications. In particular, in [5] a measurement system making use of a hybrid radar scheme with continuous wave frequency modulation and a pseudo-random code pulse techniques is discussed. They show the ability to obtain high precision information concerning the velocity of a vehicle, the distance, the direction and other useful information to improve the security in the automotive field. In [6], an experiment based on the usage of a SDRadar has been conducted to implement a multifunctional software defined unit well

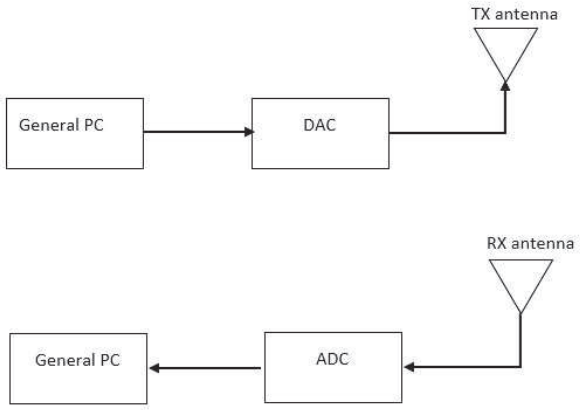

Fig. 1.1. Ideal Software Defined Radar block diagram.

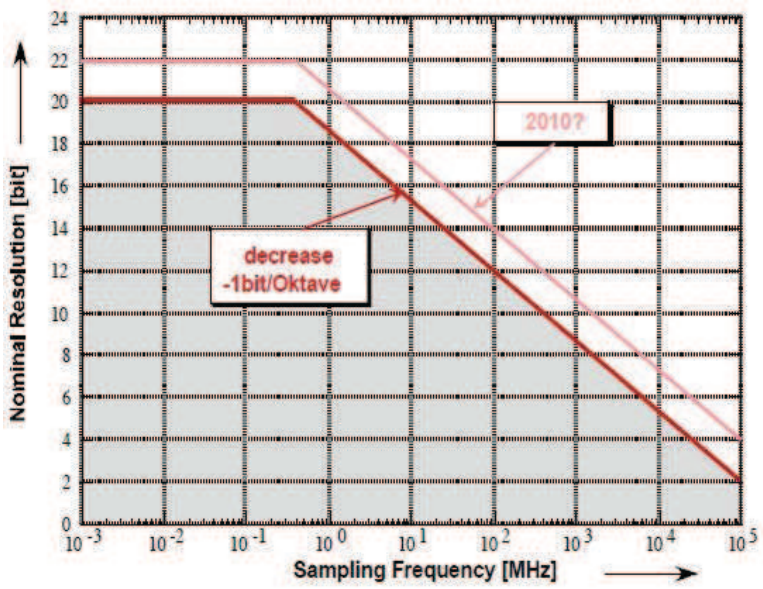

Fig. 1.2. A/D State of Art.

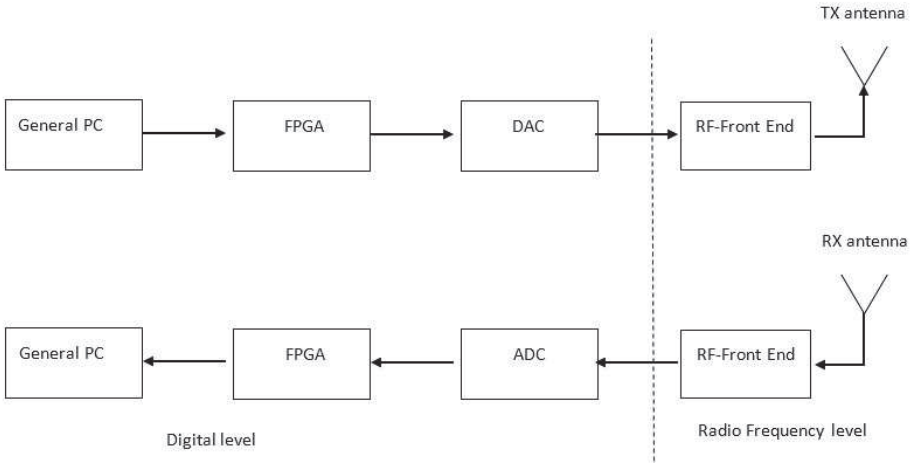

Fig. 1.3. Real Block diagram of a Software Defined Radar system.

suited for radar sensor networks, which can be used for range measurements, radar imaging and data communications. It shows important results in order to highlight the issues and the limitations related to the combination between the communication systems and the radar systems. In [7], the capability of the USRP technology is demonstrated in the realization of a passive radar by designing a low-cost DVB-T software defined system for ship detection, whilst in [8] an experiment, based on the usage of a SDRadar to implement first a basic radar system and then a synthetic aperture radar,is considered thus providing an advanced step towards the establishment of the concept of cognitive radar.

Table 1.1. Comparison of several hardware interface.

	Mbit/s	Msample/s
Fast Ethernet	100	6.25
Gigabit Ethernet	61000	62.5
USB 2.0	480	30
PCI 32-bit/33MHz	2000	125
PCI Express x1	2000	125
PCI Express x8	16000	1000
(e)SATA	2400	150

1.2 Potentialities of USRP platform in radar application

USRP is the acronym of Universal Software Radio Peripheral, it is one of the first Software defined transceiver that can be interfaced with a PC trough a software development toolkit. The first USRP motherboard was planned by Matt Ettus at the National Science Foundation" in 2006. Nowadays, several versions, each one with several features are available. In the last year, National Instruments has realized more powerful USRP boards introducing the LabView software as interface with the PC. The aim of National Instruments was to offer a good solution for the didactic and research of radio application. Recently, the use of the USRP has spread in radar field in order to realize a fledged Software Defined Radar System.

In particular,in [8] Fernandez et al. implement a SDRadar system able to transmit and receive chirp waveforms by using MATLAB and Simulink^{TM} to implement the logic blocks, to process the received data and to calculate the target range. The work in [10] presents a measurement testbed for OFDM radar which uses the USRP as a front-end.In [11], a single preliminary experimental test is performed on a big ship, and the authors themselves declare to plan more experiments on smaller ships located at further distances, in order to give a reliable validation of the proposed approach. In one of our works [12], a comparison, in radar areas, between the first generation USRP and the USRP2920 has been made, while, in [13] a first prototype of an L-band software defined radar has been realized.

1.2.1 USRP basic operation mode

In order to better understand the logic operation of a generic transceiver software defined, the basic operation mode of the platform USRP is described in this section. In figure 1.4 a classic USRP block-diagram where it is easy to locate a radio frequency stage and a digital stage is reported. The first one is composed of the power amplifier,the low noise amplifier(LNA) and the low pass filters. The digital stage,instead, is composed of the ADC and DAC converters and of the FPGA where the the digital operations of up and down conversion (DUC and DAC) for the adaptation of the stream of digital data to the interface that connect the PC takes place.

Practically,in the signal transmission path, the transmission waveform is generated by a PC through a software, then the signal is sent to the USRP

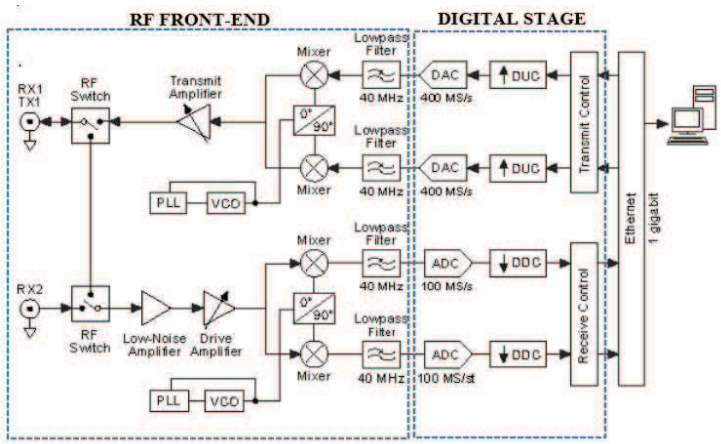

Fig. 1.4. USRP block diagram.

through the interface of connection.Once inside the USRP, the signal is directed to the FPGA where the interpolation operations (DUC) are performed. After that, the waveform is converted from digital to analogue and transferred to the RF FRONT-END for the modulation and transmission through the antenna. The signal behaviour in the reception path is analogous to that in transmission mode, but in opposite direction. The waveform received by the antenna is sent to the mixer for the IQ de-modulation and subsequently it is amplified by the LNA and filtered by Low Pass Filter. At this point, the waveform is converted from analogue to digital by the ADC and transferred to the FPGA where the decimation operation (DDC) takes place. Then, the digital signal is transferred to the PC for the post-processing.

If the desired transmitted signal is a simple $cos(2\pi f_0 t)$ where f_0 is the baseband frequency, the TX signal provided in input to the TX antenna is obtained following the scheme of the USRP internal IQ modulator reported in figure 1.5.
So starting from:

$$I = cos(2\pi f_0 t) \tag{1.1}$$

$$Q = sin(2\pi f_0 t) \tag{1.2}$$

following the scheme in figure 1.5 the TX signal will be

$$TX = Icos(2\pi f_c t) + Qsin(2\pi f_c t) =$$
$$= cos(2\pi f_0 t)cos(2\pi f_c t) - sin(2\pi f_0 t)sin(2\pi f_c t) \quad (1.3)$$

where f_c is the desired carrier frequency. Applying the addition formula of the cosine $cos(\alpha + \beta) = cos(\alpha)cos(\beta) - sin(\alpha)sin(\beta)$

$$TX = cos(2\pi f_0 t + 2\pi f_c t)$$
$$= cos(2\pi(f_0 + f_c)t) \quad (1.4)$$

In a similar manner, following the USRP internal de-modulator scheme reported in figure 1.6, the RX signal is equal to:

$$RX = A * cos(2\pi(f_0 + f_c)t + \phi) \quad (1.5)$$

where A represent the attenuation factor and ϕ is the phase term related to the propagation; the received I Q components are obtained by:

$$I_{rx} = A * cos(2\pi(f_0 + f_c)t + \phi)2cos(2\pi f_c t) \quad (1.6)$$
$$Q_{rx} = A * cos(2\pi(f_0 + f_c)t + \phi)(-2sin(2\pi f_c t)) \quad (1.7)$$

after proper mathematical steps, equation (1.6) e (1.7) become

$$I_{rx} = A * cos(2\pi f_0 + \phi) \quad (1.8)$$
$$Q_{rx} = A * cos(2\pi f_0 + \phi) \quad (1.9)$$

1.2.2 USRP bandwidth and Radar Resolution

As mentioned in the previous section, the applications of the USRP platform in radar field have been significant, providing several advantages in radar research. But, in radar systems based on USRP, the main limitation is in the bandwidth capacity of the communication interface with the host PC, as

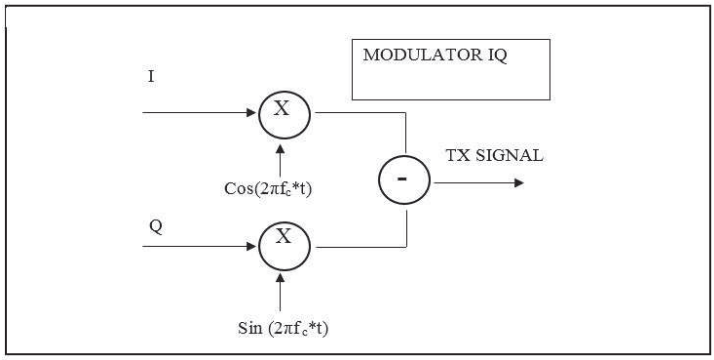

Fig. 1.5. IQ USRP internal modulator.

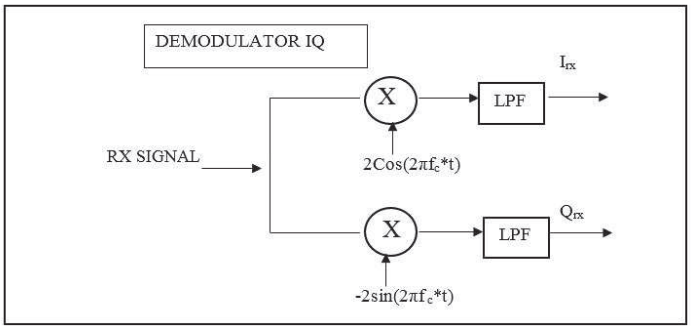

Fig. 1.6. IQ USRP internal de-modulator.

illustrated in [2],[3],[12],[13]. The bandwidth capacity of the interface, which connects the USRP to host pc, also called "host bandwidth" [14], introduces a strong limitation in the radar slant range resolution. The Ettus Research (a National Instruments Company) affirms that it is necessary to distinguish three kinds of bandwidth for the USRP platform [14] or rather :

- the analog bandwidth that represents the amount of useful bandwidth (3 dB) in the neighbourhood of the carrier frequency;
- the FPGA processing bandwidth that is the sample rate provided by the ADCs and DACs on the USRP motherboard;
- the host bandwidth that is the band capacity of the host interface that allows data to stream between the FPGA of a USRP device and a host PC.

Generally the bandwidth of a system based on the USRP is the minimum of the three kinds of band.

The radar slant range resolution denotes the capacity of the radar to distinguish two close targets; and it is calculated by the well known formula:

$$\Delta R = \frac{c}{2B} \tag{1.10}$$

where c is the speed of the light and B is the bandwidth of the radar waveform.

The host interface of first generation USRP occurs through USB 2.0 with a maximum host bandwidth of 4MHz which corresponds, using equation(1.10),to a radar resolution equal to 37.5 m. The new USRP NI2920 based on Gigabit interface presents a host bandwidth equal to 25MHz, which corresponds to a radar slant range resolution equal to 6m perfect for certain radar applications. A radar prototype based on the first USRP is discussed in [15], while in [12] a demonstration of the USRP NI2920 radar capability through open space test has been performed. The tests were conducted in order to verify the proper distance detection between the radar device and a metal plate, with dimensions equal to 1.22m 0.91 m, placed orthogonally to the direction of propagation of the radar transmitted waves. In this particular scenario, antennas are linearly polarized and the operating central frequency is equal 1.8GHz, so the device operates as an L-band radar. Specific outdoor tests have been performed on the basic system depicted in figure 1.7 and 1.8, composed by a PC, USRP 2920, and two antennas. A broadband ridged horn has been adopted as transmitting antenna, while a broadband logarithmic antenna, with the same linear polarization, has been used in receiving path. The elaboration process applied to the echo signal is a particular pulse compression technique called Stretch Processor [16].

A calibration step has been preliminarily performed without the test target, in order to characterize and subsequently remove the undesired reflections due to the open measurement environment, otherwise false peaks could be produced. The test metal plate has been subsequently placed at three different reference distances (6m, 12m, and 18 m) from the transmitting/receiving platform, in order to test the USRP NI2920 radar slant-range resolution .

The results of the processing on the received echo for different target positions is reported in figure 1.9 which, confirms the USRP NI2920 distance

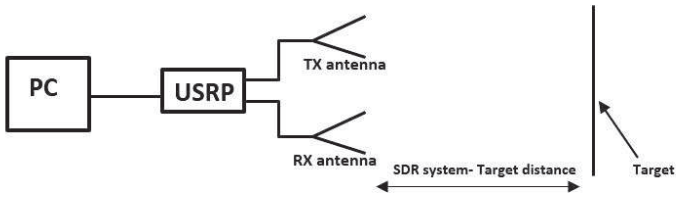

Fig. 1.7. Scheme of the basic system for outdoor test.

Fig. 1.8. Photograph of outdoor test setup.

detection capabilities and the radar slant range resolution equal to 6 m, which has thus been significantly improved in comparison with the resolution of the first generation USRP.

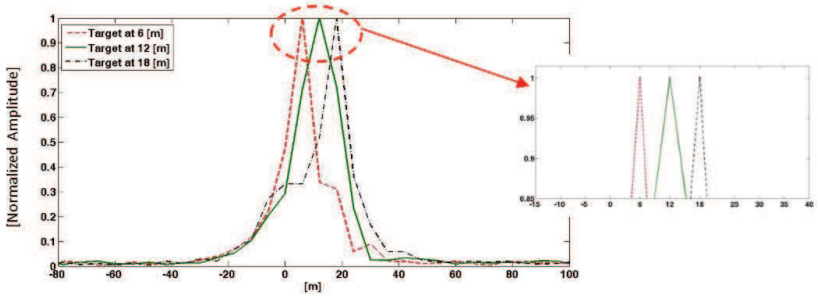

Fig. 1.9. Retrieved signal peaks for different target positions.

A similar measurement has also been conducted in anechoic chamber, positioning two test metal plates between 0m and 12m. The aim of this test is to distinguish two close targets in order to further confirm the slant range

resolution. The result of the test is shown in figure 1.10 where it is possible to observe two higher peaks corresponding to the target positions.

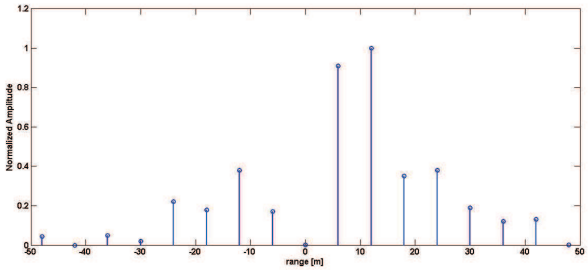

Fig. 1.10. Retrieved signal peaks with two targets placed between 0 and 12 m.

1.2.3 New Generation USRP

In this section an accurate comparison between the USRP NI 2920 and first generation USRP is reported; moreover, a brief description of newest USRP, manufactured by National Instrument, is made underlying the improvement in terms of radar slant resolution. In table 1.2 the software and hardware comparison between the two platform is shown.

Table 1.2. Comparison of several hardware interface.

	USRP	USRP2920
Software	GNU Radio or Simulink	LabView
ADC	2 channel ADC at 64MS/s	2 channel ADC at 400MS/s
DAC	2 dual channel DAC at 128MS/s	2 channel at 100MS/s
PC interface	USB 2.0	Gigabit Ethernet
FPGA	FPGA Altera Cyclone (EP1C12 Q240c8)	Xilinx Spartan-6

In order to identify the radar capability of a USRP SDRadar based system a numerical test with Additive White Gaussian Noise (AWGN)is presented. First a radar system with the USRP NI2920 is assumed and the Stretch Processor Technique (SPT) [16] is applied.

The transmitted signal is a chirp waveform:

$$s(t) = cos(2\pi(f_0 t + \frac{\mu}{2}t^2)), \qquad 0 < t < \tau \tag{1.11}$$

where μ=$\frac{B}{\tau}$ is the linear frequency-modulated coefficient, B is the system bandwidth, f_0 is the chirp start frequency and τ the chirp duration. In presence of noise the corresponding received signal is given as:

$$r(t) = \alpha s(t - \Delta t) + \omega \tag{1.12}$$

where α is the attenuation factor due to the target radar cross section, the path loss and other losses introduced by the system; Δt is the propagation delay due to the target position, and ω is the AWG noise with zero mean and variance equal to σ. In Stretch Processor the target extraction is performed by computing the Fast Fourier Transform (FFT) to the product between the transmitted signal and the received signal; the relative spectrum energy is given by:

$$A(f) =\mid F\{s(t) \cdot r(t)\} \mid^2 \tag{1.13}$$

where $F\{\bullet\}$ denotes the Fourier transform operator.

The tones present in equation (1.13) for $f = f_p$ are proportional to the target range R by the expression:

$$f_p = \frac{2BR}{c\tau} \tag{1.14}$$

The analysis conducted for the USRP NI2920 performance, in presence of white noise ω, is performed in term of the ρ parameter defined as:

$$\rho = \frac{A(f)}{A(f_{max})} \tag{1.15}$$

where:

$$A(f_{max}) = max \mid A(f_{max}) \mid: \quad f \neq fp \tag{1.16}$$

From the definition of equation (1.15) it is easy to deduce that a proper target detection can be performed for those noise parameters that guarantee the condition $\rho > 1$. Various simulation tests are performed to identify the

limit values of noise variance σ which assure a correct target position estimation. In figure 1.11, an example of proper target detection is reported by illustrating the behaviour of the spectrum energy (eq.1.13) for a target positioned at a distance equal to 18m, in presence of AWG noise with a large variance value $\sigma = 60$.

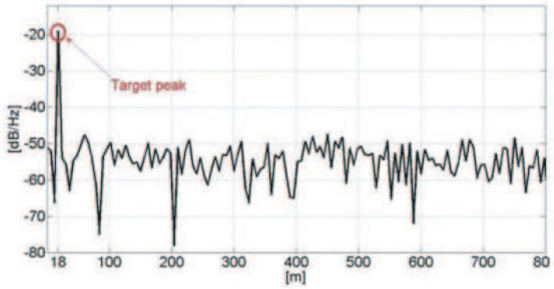

Fig. 1.11. Spectrum energy behavior in the presence of AWG noise with variance = 60 (target position = 18 m).

For the illustrated case, the parameter ρ, given by the difference between the two highest peaks (in dB), which results to be approximately equal to 27 dB, is thus strongly greater than 1 in linear scale; as imposed by the condition outlined above. Additional numerical tests of ρ parameter for different values of σ are considered, in order to obtain the graph shown in figure 1.12 where the value of ρ is maintained above the 0dB for realistic value of σ .

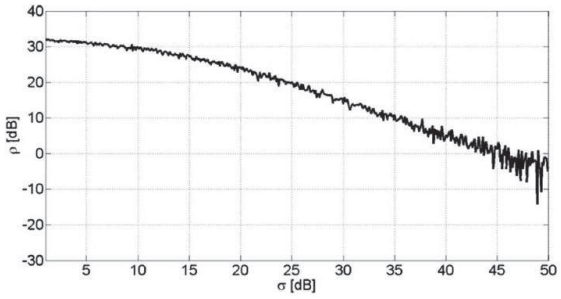

Fig. 1.12. Behavior of parameter ρ vs. variance σ (target position = 18 m).

To underline the improved target detection capabilities of SDRadar systems based on USRP NI2920, a similar noise sensitivity analysis is conducted on the conventional first generation USRP. Due to the high computational load, the SPT is practically inhibited, so in this case a time domain analysis is performed, assuming, as transmission waveform, a single pulse of duration τ :

$$s(t) = \begin{cases} A & 0 < t < \tau \\ 0 & otherwise \end{cases} \tag{1.17}$$

The received signal $r(t)$ is the same as that defined in (1.12); in this case, the target detection is performed by computing the time delay between the received and the transmitted signals. The limitations of first generation USRP are investigated, as in the previous case, by considering various simulations for different values of the noise variance σ. The results reported in figures 1.13, 1.14 and 1.15 show, on the contrary of the USRP NI2920 case, that target detection cannot be easily performed for a variance value $\sigma = 60$ (about 17 dB), thus revealing much lower range estimation capabilities.

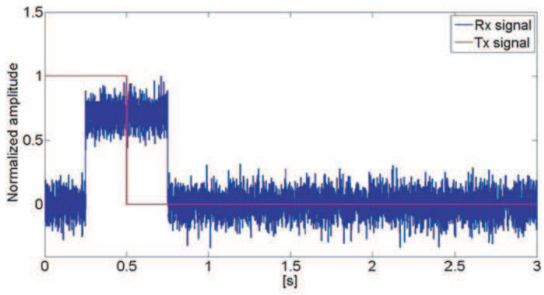

Fig. 1.13. Tx and Rx signals in the presence of AWG noise ($\sigma = 30$).

Over the NI USRP 2920, in 2013, National Instruments produced the USRP RIO (Reconfigurable Input Output).This new platform presents higher performance than NI USRP 292x series and also exists in the open source version called USRP X series produced by the Ettus Research company. The aim of the newest USRP is to improve the research in new generation wireless communication. As mentioned before, the limitation of the host bandwidth, which produces an high radar range resolution, is widely overcome due to the

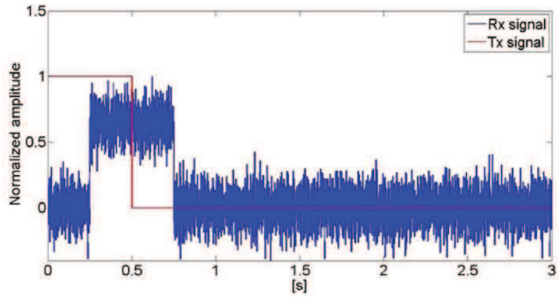

Fig. 1.14. Tx and Rx signals in the presence of AWG noise ($\sigma = 60$).

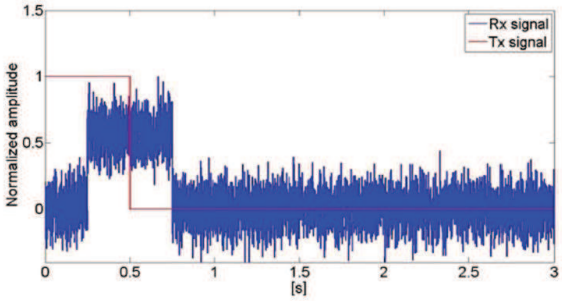

Fig. 1.15. Tx and Rx signals in the presence of AWG noise ($\sigma = 90$).

host interface PCIe (Peripheral Component Interconnect Express).The PCIe interface allows to reach 200MHz of host bandwidth, which using the equation (1.10) correspond to a radar slant range resolution equal to 0.75m. The table 1.3 summarized the main differences among the USRP version.

Table 1.3. main features of USRP version.

Features	**USRP**	**USRP NI292x**	**USRP RIO**	**USRP x SERIES**
Software	Gnu Radio	Labview	Labview	c++ or Python
Host interface	USB	Gigabit Ethernet	PCIe	PCIe
Host bandwidth	4MHz	25MHz	200MHz	200MHz
Slant resolution	37.5	6m	0.75m	0.75m
FPGA	Altera Cyclone	xlilinx Spartan-6	Kintex-7	Kintex-7
Open source	YES	NO	NO	YES

1.3 L-band Software Defined Radar Hardware Architecture

In the framework of the National Project PON01-01503 LANDSLIDE AND EARLYWARNING a Software Defined Radar system for landslide monitoring has been implemented. The first imposed goal was the possibility to create a foliage penetration radar (FOPEN Radar) [17]; this justifies the choice of the L-band as operation frequency and the horizontal polarization of the antennas. The radar system has been designed to work about 1 Km away from the target and, in order to do an areal monitoring, a mechanical scanning system has been provided.

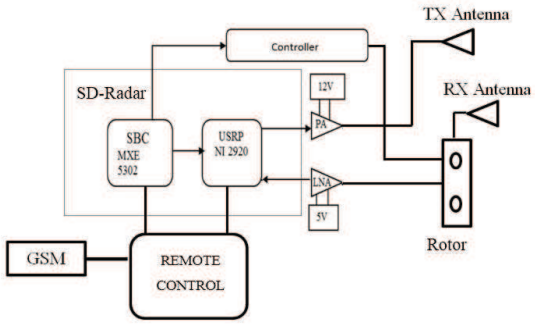

Fig. 1.16. L-band SDRadar block diagram.

In figure 1.16 a block diagram of the radar system, whose main components are described below, is reported . The SDRadar block is the central part of the instrument and consists of the SDR transceiver NI USRP NI2920 and the integrated PC MXE5302 with I5 CPU. A software LabView running on the MXE5302 manages the transmission and reception of the data and at the same time controls both the USRP NI2920 and the movement of the motor. An amplifier circuit is used to improve the radar covering, in particular a Power Amplifier with gain of 35dB at 1.8GHz is used in transmission and a Low Noise Amplifier with gain equal to 15dB take places in reception. The scanning system is composed by a Controller and a Stepped Motor on which the RX antenna is fitted; the TX antenna is a standard gain horn antenna and the RX antenna is an array composed by 8x4 elements whose design technique is proposed in [18]. A Remote Control block, composed by a single

board computer Raspberry , is connected to the SDRadar, in particular to the PC MXE 5302. This block performs a complete remote control of the radar through the internet connection due to a GSM module. Some of the remote functions are the on/off of the system and the transmission of the acquired data, via a socket connection to a possible acquisition center. The assembled L-band SDRadar system is shown in the photo reported in figure 1.17

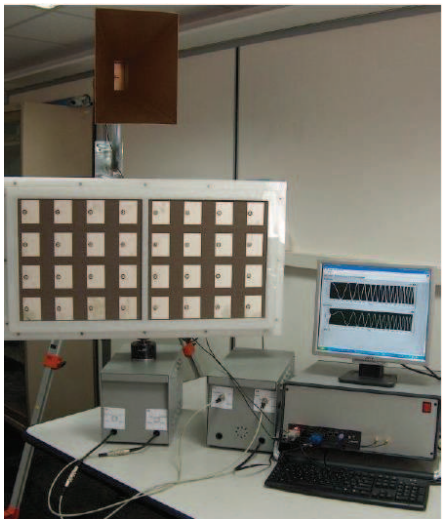

Fig. 1.17. Photograph of the L-band SDRadar system.

1.4 L-band SDRadar Software Architetture

The entire radar system is controlled by an application software written in LabView code. The software manages the transmission and the reception of the radar signal, the signal processing and the data saving. Furthermore, the rotation of the RX antenna, through the scanning system, and the client side of the remote control are also included in the LabView application software.

The software system allows to divide the area under observation in sectors, each corresponding to a scanning angle. The size of a sector depends on the distance between the radar system and area analysed. After a command received by a user or a possible data processing center (DPC) the radar system starts to work. There are two main commands, the first one is *BOC* (Begin

Outdoor Calibration); in this case the radar starts the acquisition of a scene that it is used like a reference. The second command is BAC and in this case the radar system starts the real acquisition. In both cases the system provides the transmission and the reception of the radar waveform and the signal processing for each scanning angle; when this part will be completed, all the acquired data will be sent to the DPC. The diagram reported in figure 1.18 describes the algorithm and the software architecture. In the remaining part of this section the signal processing algorithm, the remote control operation and the data saving are discussed in detail.

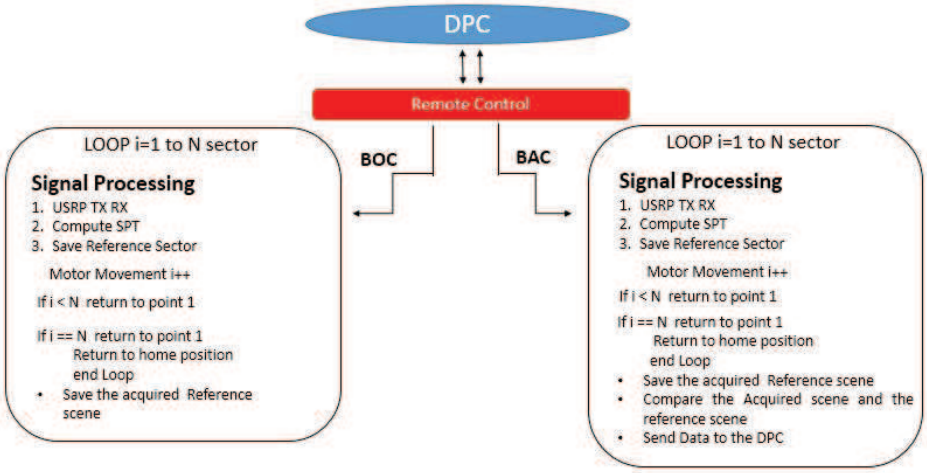

Fig. 1.18. Software algorithm.

1.4.1 Signal Processing Technique

The radar signal processing chosen is a particular compression technique called Stretch Processor [19]. This processing technique consists of the following steps: first, the radar returns are mixed with a replica (reference signal) of the transmitted waveform. This is followed by Low Pass Filtering (LPF); next, Analog to Digital (A/D) conversion is performed; and finally, the Fast Fourier Transform is used in order to extract the tones that are proportional to the target ranges, since stretch processing effectively converts time delay into frequency. Figure 1.19 summarizes the technique.

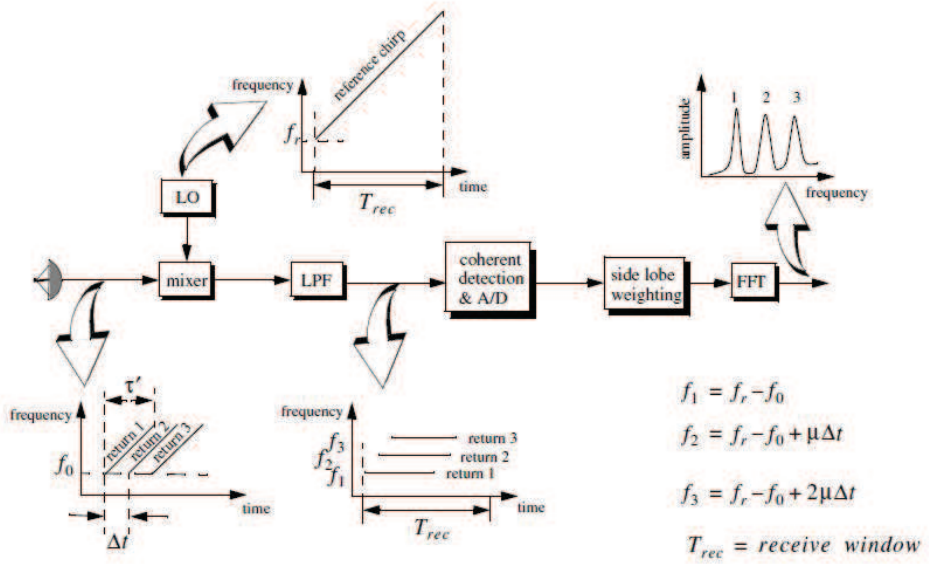

Fig. 1.19. Block diagram of Stretch Processor technique.

The transmitted waveform is a chirp signal that can be expressed by the following equation.

$$s(t) = cos(2\pi(f_0 t + \frac{\mu}{2}t^2)), \qquad 0 < t < \tau' \tag{1.18}$$

where f_0 is the chirp start frequency and $\mu = \frac{B}{\tau'}$ is the LFM coefficient that depends on the signal bandwidth B and on the chirp duration τ'.

Assuming a point scatterer at range R, the radar received signal will be:

$$r(t) = acos\left[2\pi(f_0(t - \Delta\tau) + \frac{\mu}{2}(t - \Delta\tau)^2\right] \tag{1.19}$$

where a is related to the radar cross section (RCS) and $\Delta\tau$ is the propagation delay proportional to the target distance R equal to $R = \frac{c\Delta\tau}{2}$ where c is the speed of the light.

Considering a reference signal like:

$$s_{ref} = cos(2\pi(f_0 t + \frac{\mu}{2}t^2)), \qquad 0 < t < T_{rec} \tag{1.20}$$

where T_{rec} is the receiving window defined as:

$$T_{rec} = \frac{2(R_{max} - R_{min})}{c} = \frac{2R_{rec}}{c} \tag{1.21}$$

with R_{max} and R_{min} equal to the minimum and the maximum range measurable by the radar system.

After the mixing of the echo signal (eq. 1.19), and the replica (eq. 1.20) and after the low pass filter operation used in order to avoid the high frequency products by the mixer, the signal will be:

$$s_0(t) = acos(2\pi f_0 \Delta\tau + 2\pi\mu\Delta\tau t - \pi\mu(\Delta\tau)^2) \tag{1.22}$$

Substituting $\Delta\tau = \frac{2R}{c}$ into eq (1.22) and collecting the terms:

$$s_0(t) = acos\left[(\frac{4\pi BR}{c\tau'})t + \frac{2R}{c}(2\pi f_0 - \frac{2\pi BR}{c\tau'})\right] \tag{1.23}$$

assuming $\tau' >> \frac{2R}{c}$ eq. 1.23 can be approximated by:

$$s_0(t) = acos\left[(\frac{4\pi BR}{c\tau'})t + \frac{4\pi R}{c}f_0\right] \tag{1.24}$$

The instantaneous frequency is:

$$f_{inst} = \frac{1}{2\pi}\frac{d}{dt}\left[(\frac{4\pi BR}{c\tau'})t + \frac{4\pi R}{c}f_0\right] = \frac{2BR}{c\tau'} \tag{1.25}$$

which clearly indicates that the target range is proportional to the instantaneous frequency.

Therefore applying a proper FFT to the mixed signal, a peak at generic frequency f_1 indicates the presence of a target at range:

$$R_1 = f_1\frac{c\tau'}{2B} \tag{1.26}$$

The same analysis can be performed considering N targets; in this case, the total received signal, after the mixer and the LPF operation, is equal to:

$$\sum_{i=1}^{N} a_i cos\left[\left(\frac{4\pi BR_i}{c\tau'}\right)t + \frac{2R_i}{c}\left(2\pi f_0 - \frac{2\pi BR_i}{c\tau'}\right)\right] \tag{1.27}$$

And hence,observing the equation above, the target returns appear at constant frequency tones that can be resolved using the FFT. The frequency resolution can be computed using the following procedure: considering two adjacent point scatterers at range R_1 R_2, the minimum frequency separation, Δf, between those scatterers can be computed from eq. (1.25), so that they are resolvable; more precisely,

$$\Delta f = f_2 - f_1 = \frac{2B}{c\tau'}(R_2 - R_1) = \frac{2B}{c\tau'}\Delta R \tag{1.28}$$

furthermore, substituting the range resolution equation $\Delta R = \frac{c}{2B}$ in eq.(2.1):

$$\Delta f = \frac{2B}{c\tau'}\left(\frac{c}{2B}\right) = \frac{1}{\tau'} \tag{1.29}$$

The maximum resolvable frequency by the FFT is limited in the region $\pm\frac{N\Delta f}{2}$ since, considering the receiving window

$$\frac{N\Delta f}{2} > \frac{2B(R_{max} - R_{min})}{c\tau'} = \frac{2B}{c\tau'}R_{rec} \tag{1.30}$$

and substituting eq. (1.21) and (1.29) in eq. (1.30), the number of sample N must chosen respecting the following equation.

$$N > 2BT_{rec} \tag{1.31}$$

In order to implement the SPT in the SDRadar system the adaptation of the tx signal to the NI USRP hardware is necessary. The tx signal, expressed in eq.(1.18) ,is a bandpass signal or rather, a modulated waveform; while, the NI USRP 2920 admits in input baseband waveform . To obtain the signal $s(t)$ at the output of the IQ modulator of the NI USRP2920 a little mathematical elaboration and I e Q components calculation are necessary.

The signal in eq. (1.18) can be expressed as:

$$s(t) = cos(2\pi(f_0 t + \frac{\mu}{2}t^2)) = cos(2\pi f_0 t + \pi\mu t^2) \tag{1.32}$$

following the IQ modulator scheme in figure 1.5 and according to the equation (1.3) the easiest choice for I e Q can be:

$$I = cos(\pi\mu t^2) \tag{1.33}$$

$$Q = sin(\pi\mu t^2) \tag{1.34}$$

providing eq. (1.33) and (1.34) like input to eq.(1.3), the signal $s(t)$ is obtained.

$$s(t) = cos(\pi\mu t^2)cos(2\pi f_0 t) + sin(\pi\mu t^2)sin(2\pi f_0 t)$$

$$s(t) = cos(2\pi(f_0 t + \frac{\mu}{2}t^2)) \tag{1.35}$$

The chirp signal used in transmission, imposing the IQ carrier frequency f_0 equal to 1.8GHz, is shown in figure 1.20.

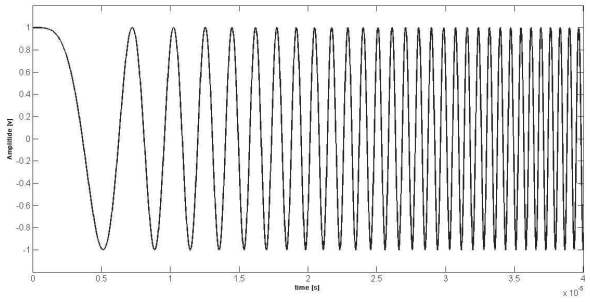

Fig. 1.20. TX signal.

1.4.2 Remote Control

The remote control system is an optional block that allows the complete remote control of the L-band radar system. This block is composed by the single board computer Raspberry, a modem 3G and a Relay (see Fig 1.21); the latter is used to interrupt the power and turn completely the radar system off. The modem 3G is used for the transmission of the acquired data to a possible DPC and the reception of the commands. The whole process is controlled by a software running on the SBC Raspberry. Substantially the Remote Control block is a middleware between the L-band SDRadar System and a Digital Processing Center. To enable the communication between the radar system

and the Digital Processing Center a communication protocol has been implemented. This protocol is summarized in figure 1.22; in particular, the scheme is the implementation of the states and the actions taken by the entire system according to the commands exchanged between the client side,implemented on the SDRadar system in LabView code, and the server side implemented on the SBC Raspberry. In order to better understand the protocol in figure 1.23 the time line message is reported.

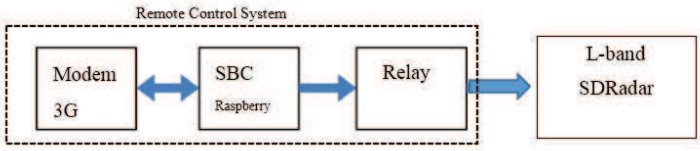

Fig. 1.21. Remote control system block diagram.

Description of the state

- **Ready**: this state is assumed at the beginning of the session, in this state the system is in a listening position of the possible commands;
- **BOC**(Begin Outdoor Calibration) this state is assumed as the consequence of the command exchanges $BOC-BOCSTARTEDBOC-END$; in this state the acquisition and the broadcast of a reference scene is performed.
- **BAC**(Begin Acquisition) this state is assumed as the consequence of the command exchanges $BAC-BACSTARTEDBOCEND$; in this state the acquisition and the broadcast of a measure scene is performed.

1.4.3 Data Acquisition and Saving

The measure file given in output by the radar system is the result of the Stretch Processor applied for each scanning angle; practically, the system produces a measure file for each sector which corresponds to one red ellipse referring to the figure 1.24

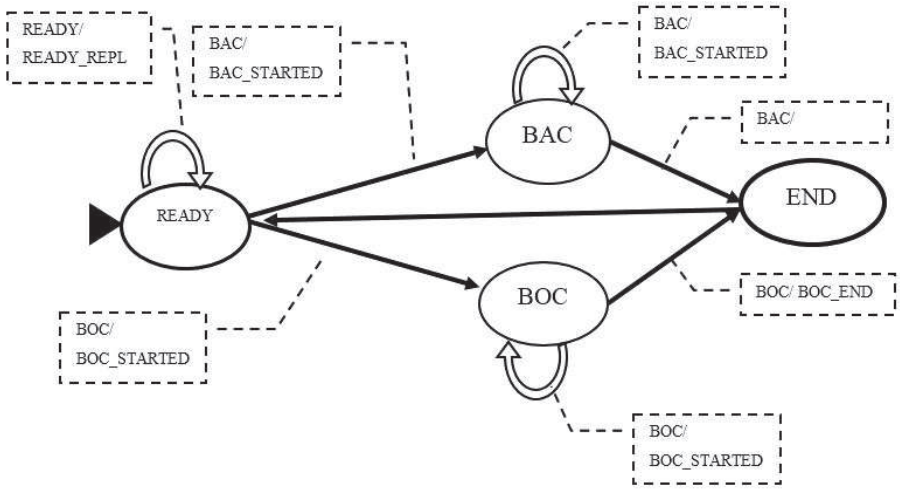

Fig. 1.22. State machine of the system.

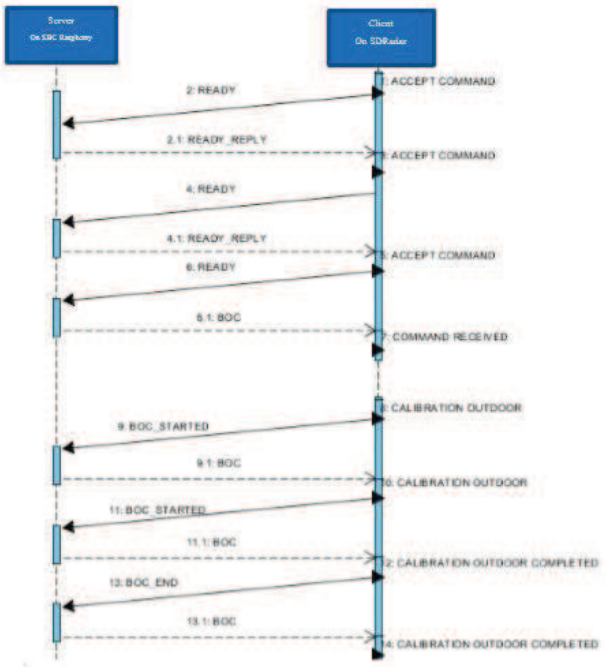

Fig. 1.23. Time line message of the protocol.

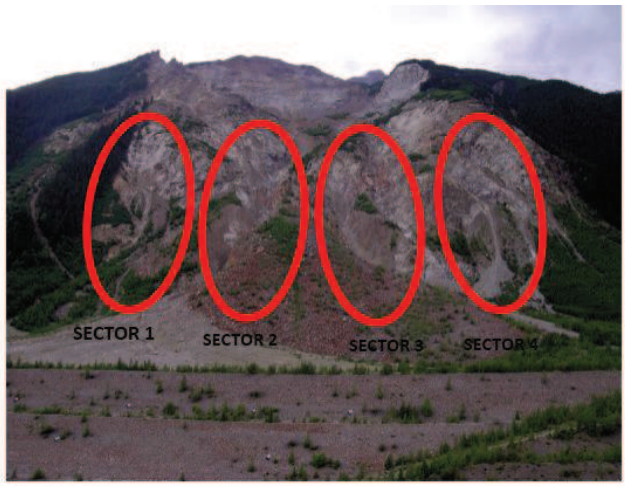

Fig. 1.24. division of the scene under observation in sector.

In order to verify the data correctness, the measure file also includes the transmitted signal, the received signal, the SPT results for the reference scene and the difference between the reference and the acquired scene. Therefore the output file is a .txt file composed by eight columns described below:

- **RANGE**: axis distances;
- **FFT MEASURE**: SPT output relative to the measured sector;
- **DIFF**: difference between the normalized FFT MEASURED and the normalized FFT CALIBRATION;
- **T TX** time domain tx signal relative to the measured sector;
- **T RX** time domain rx signal relative to the measured sector;
- **FFT CALIBRATION** SPT output relative to the reference sector;
- **TX CAL** time domain tx signal relative to the reference sector;
- **RX CAL** time domain rx signal relative to the reference sector

In order to reduce the load of data transmitted to a possible data processing center, the measure file is strongly reduced; in particular, the file includes only the column relative to the SPT OUTPUT resized to the useful range for each sector. A possible format of the reduced measure file suitable for the transmission is shown in figure 1.25

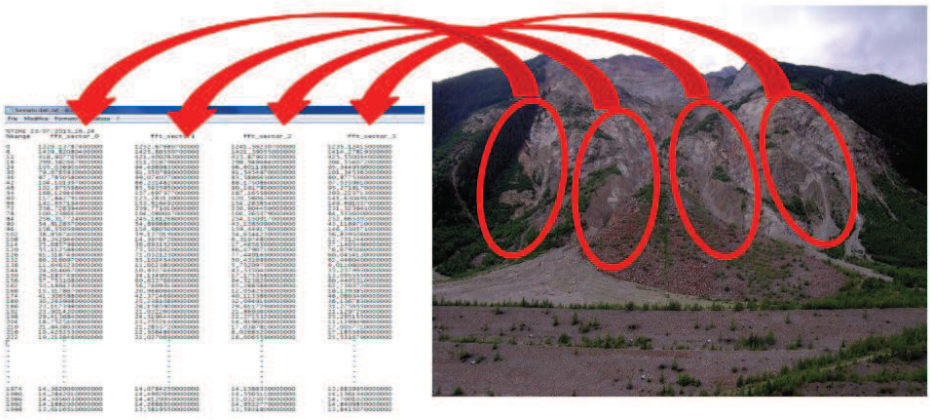

Fig. 1.25. Example of a measure file.

1.5 Experimental Validations

Specific outdoor and indoor tests with L-band SDRadar platform have been performed in order to validate the entire assembled system. In both case a metal plate has been adopted as reference target and placed at different distances from the transmitting/receiving platform. Both tests have been conducted for only one sector, therefore without the use of the mechanical scanning system; furthermore, before starting the tests, an internal calibration of the system, connecting the TX RX port with a cable long 50cm, has been made in order to detect the NI USRP2920 internal delay. The indoor test has been conducted in the anechoic chamber, the setup is depicted in the photograph shown in figure 1.26.

During the test the metal plate has been placed at several distances between 0m and 12m the test has been conducted initially using only one target and subsequently using two targets in order to verify the radar slant resolution. The transmitted signal,expressed by eq.1.18, has been considered with a band B equal to 25MHz, f_0 equal to 1.8GHz, a chirp duration τ of about 0.6 ms and a receiving window $Trec$ equal to τ. The exact and software retrieved target positions for different target distances are reported in Table 1.4 while, in the graph in figures 1,27 ,1.28 and 1.29 the SPT results are shown.

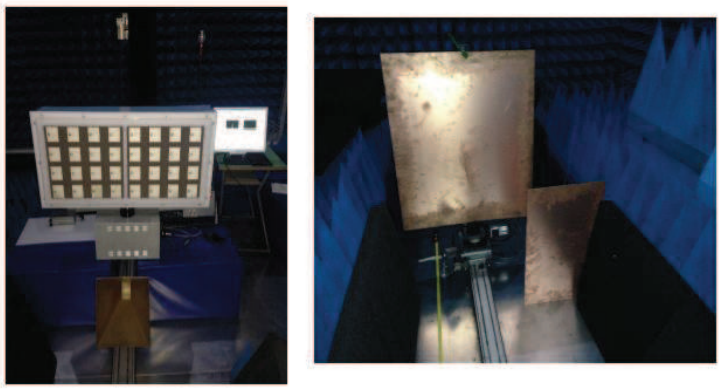

Fig. 1.26. L-band SDRadar system during the anechoic chamber test (on left), metal plate target (on right).

Table 1.4. Exact and Software target position.

Num of Target	Target Position [m]	SPT output [m]
1	0 ÷ 6	6
1	6 ÷ 12	12
2	0 ÷ 12	6-12

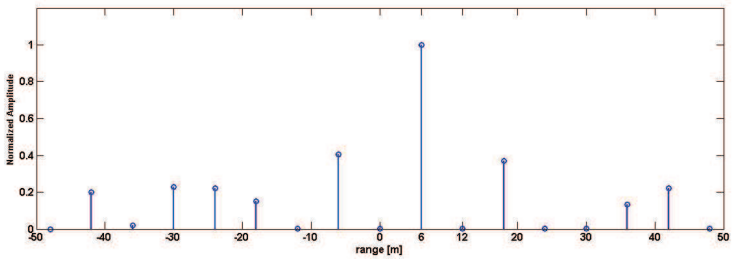

Fig. 1.27. SPT output with one target placed between 0 ÷ 6m.

The outdoor experimentation has been conducted in order to perform a more complete test. In this case, the capacity of the SDRadar to detect metal plate at farther distances than in anechoic chamber, the foliage penetration and radar behaviour when the antenna is oriented towards a multiple target area have been verified, The measurement setup for outdoor tests is reported in figure 1.30; during the test a broadband ridged horn has been adopted as

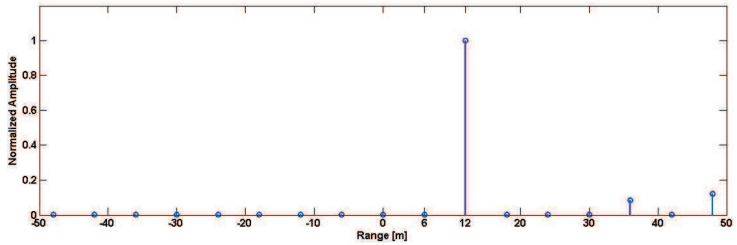

Fig. 1.28. SPT output with one target placed between 6 ÷ 12m.

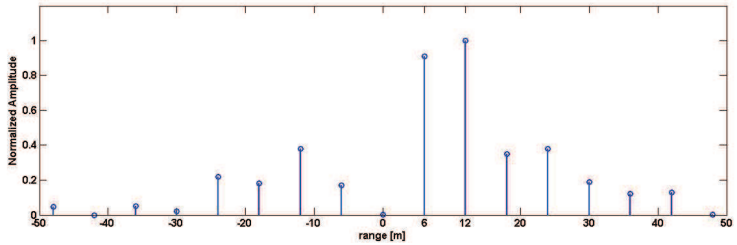

Fig. 1.29. SPT output with two targets placed between 0 ÷ 12m.

transmitting antenna, while a broadband logarithmic antenna has been used in the receiving path.

Fig. 1.30. Photograph of the L-band SDRadar system during the outdoor experimentation.

Table 1,5 reports the real and software retrieved target position, while the graphs in the figures 1.31 to 1.35 show the signal processing output.

Table 1.5. Exact and software retrieved target position

Num of Target	Target Position [m]	SPT output [m]
1	15 ÷ 30	24
1	30 ÷ 40	42
1	50 ÷ 60	54
2	15 ÷ 30	18-24
2	20 ÷ 30	24-30
2	30 ÷ 40	30-36

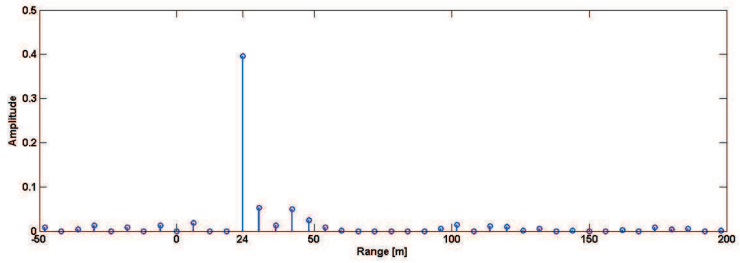

Fig. 1.31. SPT output with one target placed between 15m and 30m.

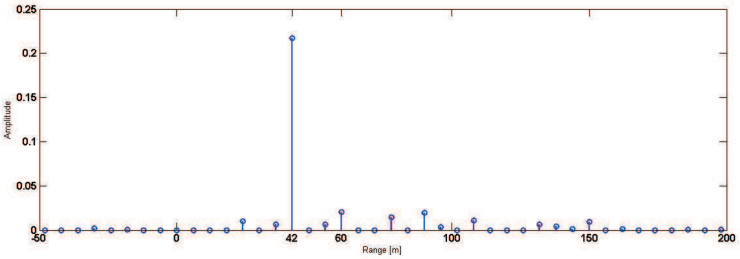

Fig. 1.32. SPT output with one target placed between 30m and 40m.

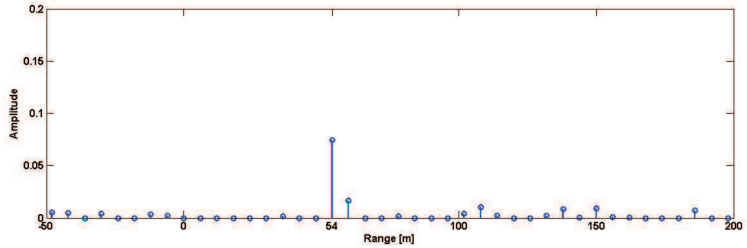

Fig. 1.33. SPT output with one target placed between 50m and 60m.

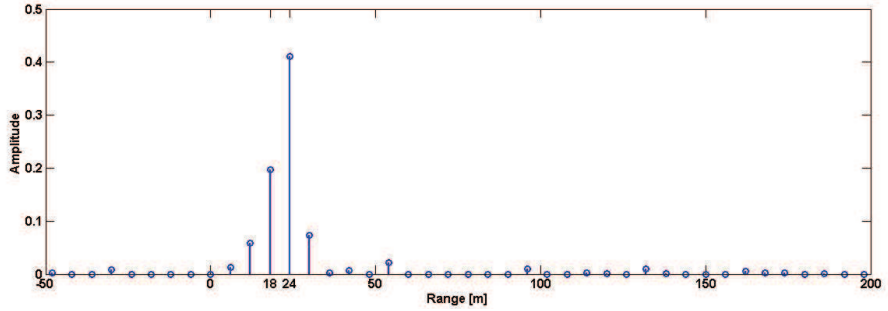

Fig. 1.34. SPT output with two targets placed between 15m and 30m.

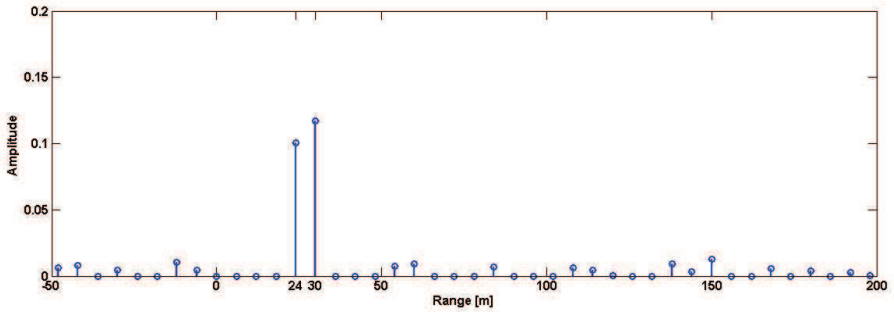

Fig. 1.35. SPT output with two targets placed between 20m and 30m.

To verify the foliage penetration capability of the L-band SDRadar the metal plate has been hidden behind a vegetation layer; the target detection is shown is figure 1.37. In the graph in figure 1.38, the SDRadar behaviour, with the TX and RX antennas pointed towards a traffic zone is reported.

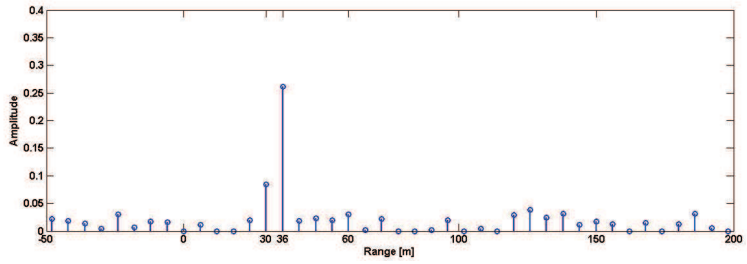

Fig. 1.36. SPT output with two targets placed between 30m and 40m.

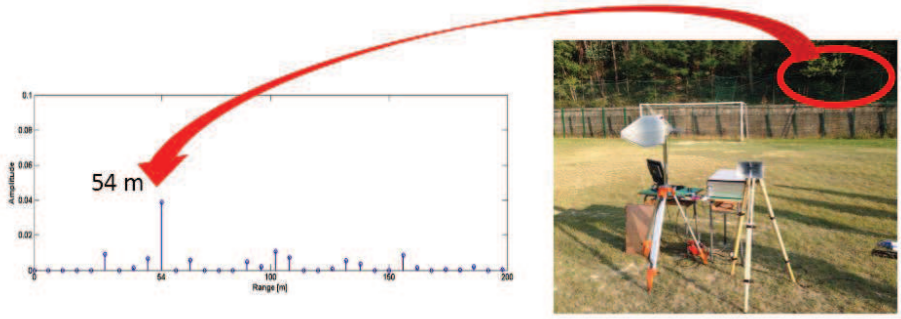

Fig. 1.37. SPT output with the target hidden behind a vegetation layer.

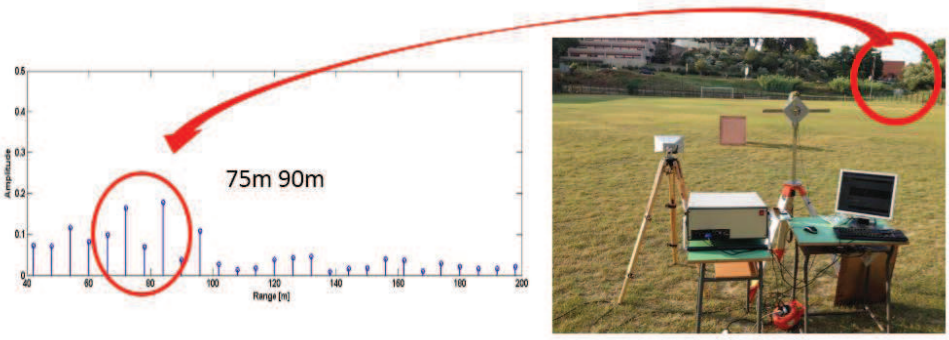

Fig. 1.38. SPT output of a traffic zone.

1.6 Conclusion

In the first section of this thesis the implementation of L-band SDRadar has been discussed. A low cost, flexible, compact and versatile solution to create high performance radar systems has been proposed; furthermore, the potentialities of the USRP NI2920 platform have been adopted to realize a SDRadar system giving a 6m of slant range resolution. The work wants to underline the capabilities of the Software Radio transceiver in radar field highlighting the main benefits of a Software Defined Radar system. The entire implementation is part of the National Project *"LANDSLIDE AND EARLYWARNING"* and won the first prize at *NI Aerospace and Defense Forum 2013* international conference organized by National Instruments.

2

Software Defined Measurement for soil Electrical Properties

2.1 Introduction

In this chapter an application of the Software Defined system potentialities for soil electrical properties detection is presented. This work wants to emphasize the hardware reuse of a SDR system as its main characteristic; in fact, this benefit gives the possibility to create a *Multipurpose Radar system* or rather, several systems like Doppler,GPR or FOPEN Radar in a single hardware; in order to produce a significant reduction in costs. The dielectric properties of materials are strongly influenced by several different factors, such as frequency, temperature and homogeneity. As a consequence of this, no single technique can be assumed to perform an accurate dielectric characterization at all frequency bands and loss conditions [20]. A special challenge occurs in the dielectric measurement of thin materials, usually adopted in microstrip structures, where the uncertainty of the retrieving procedure significantly increases [21].

Existing methods for the dielectric characterization, based on cavity resonators, coaxial probes, striplines [22] or open-resonators [23], usually adopt expensive vector network analyzers to perform the scattering parameter measurements. Furthermore, depending on the specific material and application, the retrieving procedures require dedicated hardware and software, thus increasing the overall cost of the test setup.

Electromagnetic sensors, such as Ground Penetrating Radar (GPR), are largely adopted for the detection of buried land mines, unexploded ordnance and soil discontinuities. The performance of these sensors strongly depend

on the dielectric properties of the soil, which in turn are related to specific parameters, such as texture, bulk density, and water content. The accurate knowledge of soil dielectric constant is of primary importance in this kind of radar application, and particular difficult to achieve in the presence of dispersive media, where the dielectric properties vary with frequency.

The use of a multi-band radar technique is here considered to focus this problem; in particular, a multi-band SDR technology is proposed to implement an algorithm in order to perform an accurate soil discontinuities detection. Furthermore, the adoption of Orthogonal Frequency-Division Multiplexing (OFDM) radar signal processing technique [24] is discussed to implement the multi-band system able to retrieve the frequency variation of soil permittivity. The results of the numerical simulation are compared with the empirical models discussed in [25] [26] [27] and reported in the following sections.

2.2 OFDM Radar Algorithm

The radar signal processing technique proposed is based on the transmission of OFDM signal. This particular waveform has allowed the study of systems able to do both radar detection and communication (RADCOM)[28] [29]. Before introducing, the Software Defined Measurement (SDM) idea the basic principle of OFDM radar processing is presented following the approach proposed in [30] [31] [32]. The modulation OFDM is generally used for the data transmission and only recently it has also been used in radar field. The OFDM modulation is a combination of modulation and multiplexing techniques, which allows the transmission of complex modulation symbols obtained through discrete phase modulation (e.g. BPSK). The block diagram of the TX signal generation is shown in figure 2.1.

The symbols $S_i(t)$,which can be equal to 1 or -1, are modulated with N orthogonal subcarrier with duration T, the subcarrier are frequency spaced by the interval:

$$\Delta f = \frac{1}{T} \tag{2.1}$$

this condition is necessary in order to guarantee the orthogonality.

Therefore the modulated symbols can be expressed as

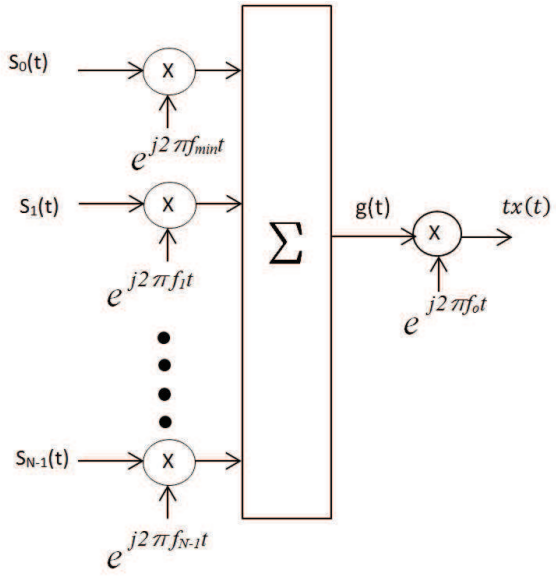

Fig. 2.1. OFDM TX signal generation.

$$\psi(t) = S_i(t)e^{j2\pi(f_i)t} \tag{2.2}$$

where:

$$f_i = f_{min} + k\Delta f, \qquad k = 0, 1, 2, ...N - 1 \tag{2.3}$$

with f_{min} giving the minimum frequency with an arbitrary value. The baseband signal $g(t)$ is obtained from the multiplexing operation

$$g(t) = \sum_{i=0}^{N-1} S_i(t)e^{j2\pi(f_i)t}, \qquad 0 < t < T \tag{2.4}$$

an example of the signal g(t) obtained using 4 symbols modulated on 15 subcarriers with a $\Delta f = 40KHz$ is reported in figure 2.2, generally a guard time Tg is considered between one symbol and the other in order to avoid the *inter-symbol interference* (ISI).

The signal provided in input to the TX antenna is obtained modulating the signal $g(t)$ at frequency f_0:

$$tx(t) = g(t)e^{j2\pi f_0 t} \tag{2.5}$$

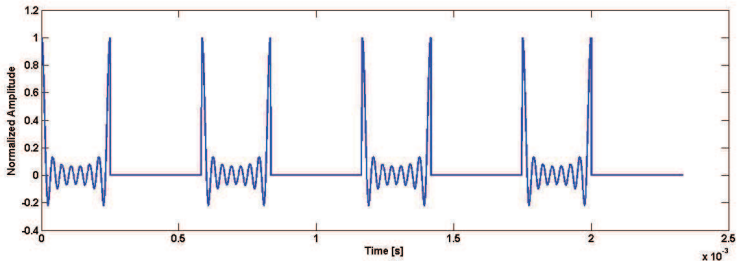

Fig. 2.2. $g(t)$ signal with M=4 symbol modulated on N=15 subcarriers with a Δf = 40KHz

An OFDM radar works as a static system, by transmitting a signal like eq. 2.5 and receiving reflection of this signal from targets in the path of the signal wavefront. The received signal, in absence of Doppler effect, can be expressed as:

$$rx(t) = \sum_{k=0}^{h-1} b_h g(t - \tau_h) e^{j2\pi f_0 (t-\tau_h)} \tag{2.6}$$

where H is the number of reflecting targets, τ_h is the propagation delay related to the target position d_h and b_h is the attenuation factor related to the Radar Cross Section and Pathloss. The OFDM signal processing technique [24] gives an unambiguous range equal to:

$$d_{unamb} = \frac{c}{2\Delta f} = \frac{cT}{2} \tag{2.7}$$

where c is the speed velocity. The radar slant range resolution that depends on the total bandwidth B occupied by the transmitted signal is expressed by:

$$\Delta R = \frac{c}{2B} = \frac{c}{2N\Delta f} \tag{2.8}$$

Figure 2.3 shows the operation mode of the OFDM Radar signal processing [33]; the baseband transmitted signal is composed by M symbols $S_i = [S_0, S_1, S_2, ...S_{M-1}]$ modulated with N orthogonal frequencies $[f = f_{min}, f_{min} + \Delta F, f_{min} + 2\Delta F ... + f_{min} + (N-1)\Delta F]$ using OFDM modulation. The received baseband signal is obtained after the OFDM demodulation of the signal $Rx(t)$ expressed by the equation 2.6 and it can be represented as the vector of the received symbols, $Y_i = [Y_0, Y_1, Y_2 ... Y_{m-1}]$. The target position

is then retrieved by applying the IFFT (Inverse Fast Fourier Transform)on the result of the wise division among the symbols received Y and the symbols transmitted S.

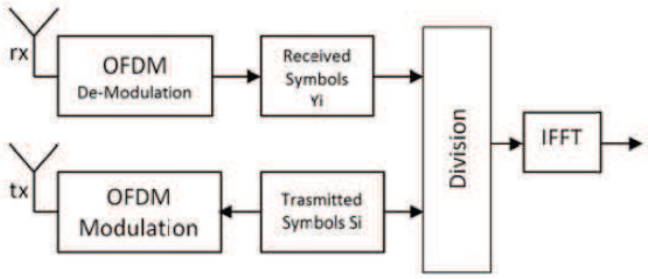

Fig. 2.3. OFDM radar processing

Another way to express the TX signal is in matrix form proposed in [24]. The transmitted matrix F_{tx} is composed by N rows, corresponding to N subcarriers, and by M column which correspond to M symbols.

$$F_{tx} = \begin{pmatrix} c_{00} & c_{01} & \cdots & c_{0M-1} \\ c_{10} & c_{11} & \cdots & c_{1M-1} \\ \vdots & \vdots & \ddots & \vdots \\ c_{N-10} & c_{N-11} & \cdots & c_{N-1M-1} \end{pmatrix} \tag{2.9}$$

The OFDM modulated TX signal is obtained as follows:

$$tx(t) = F_{tx} W_{MxK} e^{j2\pi f_0 t} \tag{2.10}$$

where W_{MxK} is the subcarrier matrix with M symbols and K samples that represent the symbol duration.

In this case the result of the demodulation of the $rx(t)$ signal is a symbol matrix Y_{rx}.

The IFFT applied on the rows of the matrix, which is obtained dividing the RX and TX matrix, gives information on the target position; while, the FFT applied on the column give information on the target velocity [24].

$$Target\ Distance = IFFT\left(\frac{Y_i}{S_i}\right) \tag{2.11}$$

$$Target\ Velocity = FFT\left(\frac{Y_j}{S_j}\right) \tag{2.12}$$

Figure 2.4 shows the results of the OFDM signal processing for three stationary targets positioned in 18m 35m and 180m. The numerical analysis has been conducted considering a number of subcarrier N=511, a number of symbols M=11 and $\Delta f = 500$KHz and then with a radar slant range resolution equal to $\Delta R = \frac{c}{2N\Delta f} = 0.58m$

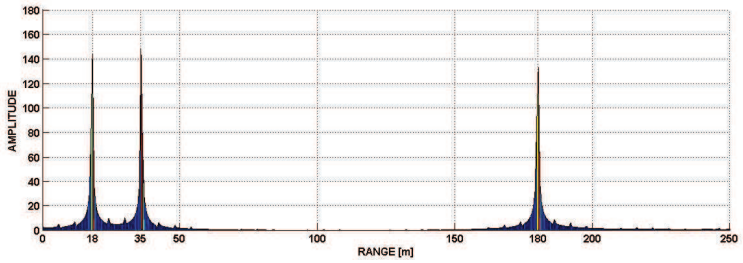

Fig. 2.4. Result of the OFDM radar processing

2.3 Empirical Models for Soil' Dielectric Properties

The dielectric properties of a soil depend on a number of factors, such as bulk density, sand and clay percentage of soil particles, volumetric water content, temperature and frequency of interest [25]. In this section two empirical models, discussed in [25] [26] [27], for the soil's dielectric properties are presented. These two empirical models will be used in the next section in order to validate and compare the results of the numerical analysis on the Software Defined Measurement platform, presented in the next section. The first model is adapted for the frequency range between 1.4GHz and 18GHz, while the second one is calibrated for the frequency range between 0.3GHz and 1.4GHz The models calculate the real and the imaginary part of the dielectric constant ϵ of a particular soil, on the base of the following inputs.

- θ: volumetric water content;

- f : operating frequency;
- S : fraction of sand particles;
- C : fraction of clay particles;
- ρ_s: density of soil particles (typically $2.66 g/cm^3$)
- ρ_b: bulk density of the soil (typically $1.66 g/cm^3$)
- $\epsilon_{fw} = \epsilon'_{fw} + j\epsilon''_{fw}$: dielectric constant of free water.

In the first model ($1.3GHz \div 18GHz$) [25] the dielectric constant computation is based on the equation of the soil conductivities expressed as follows:

$$\sigma_{eff} = -1.645 + 1.929\rho_b + 2.013S + 1.594C \tag{2.13}$$

the β' and β'' parameters that take into account the sand and clay particles;

$$\beta' = 1.2748 - 0.519S - 0.152C \tag{2.14}$$

$$\beta'' = 1.33797 - 0.603S - 0.166C \tag{2.15}$$

and the dielectric constant of free water:

$$\epsilon_{fw} = \epsilon'_{fw} + j\epsilon''_{fw} \tag{2.16}$$

with

$$\epsilon'_{fw} = \epsilon_{w\infty} + \frac{\epsilon_{w0} - \epsilon_{w\infty}}{1 + (2\pi f \tau_w)^2} \tag{2.17}$$

$$\epsilon''_{fw} = \frac{2\pi f \tau_w (\epsilon_{w0} - \epsilon_{w\infty})}{1 + (2\pi f \tau_w)^2} + \frac{\sigma_{eff}}{2\pi\epsilon_0 f} + \frac{(\rho_s - \rho_b)}{\rho_s^\theta} \tag{2.18}$$

where :

- ϵ_0: dielectric constant in free space;
- ϵ_{w0} dielectric constant of water (equal to 80.1 at 20 Celsius);
- $\epsilon_{w\infty}$: maximum limit of free water equal to 4.9;
- τ_w relaxation time of water equal to $9.23 \cdot 10^{-12}$;

On the basis of the previously equation, the authors in [25] [26] [27] obtain a formula for the soil dielectric constant expressed in real part and imaginary part $\epsilon = \epsilon' + j\epsilon''$ where:

$$\epsilon' = \left[1 + \frac{\rho_s}{\rho_b}(\epsilon_s^\alpha - 1) + \theta^{\beta'}\epsilon_{fw}^\alpha + \theta\right]^{\frac{1}{\alpha}} \tag{2.19}$$

$$\epsilon'' = \left[\theta^{\beta''}(\epsilon_{fw}'')^\alpha\right]^{\frac{1}{\alpha}} \tag{2.20}$$

where α is equal to 0.65 and the dielectric constant of the soil particles $\epsilon_s = (1.01 + 0.44\rho_s)^2$. For the second model, between 0.3GHz and 1.3GHz, the soil dielectric constant is obtained in a similar way, except for the soil conductivity that in this case is equal to:

$$\sigma_{eff} = 0.0467 + 0.2204\rho_b - 0.4111S + 0.6614C \tag{2.21}$$

In figure 2.5 the plot of the real and imaginary part of the dielectric constant respect to the water content θ at 900MHz is reported, while in figure 2.6 the plot of the dielectric constant behaviour respect to the frequency is shown; the discontinuities in the graph are due to the use of two different models.

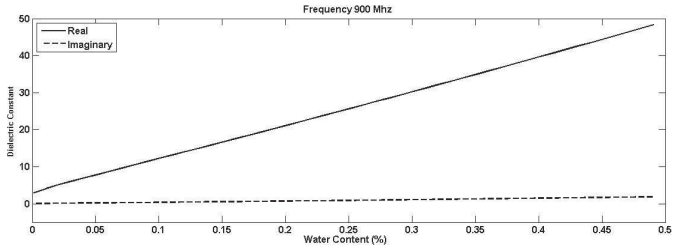

Fig. 2.5. Dielectric constant behaviour vs. the water content at 900MHz.

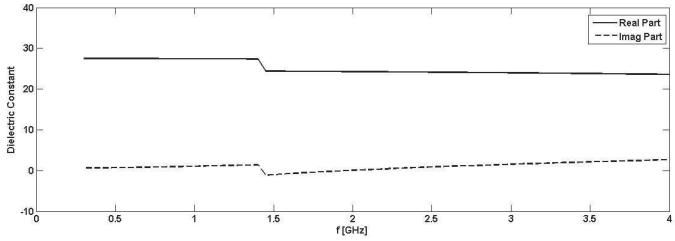

Fig. 2.6. Dielectric Constant behaviour vs. the frequency

2.4 Multi Band OFDM SDR

In order to obtain a multi-band configuration of the SDR system the original scheme,reported in figure 2.1, must be modified. The idea is the adoption of M carrier frequencies $f_0, f_1, f_2 ... fm - 1$ so the new scheme of the multi-band OFDM is shown in figure 2.7.

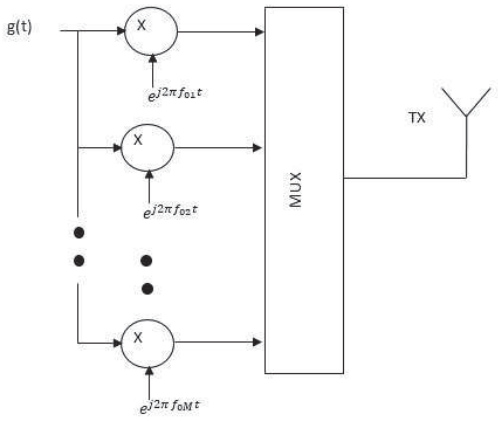

Fig. 2.7. Block diagram of OFDM multi-band Radar System

Following the scheme in figure 2.7 there are two possible ways to implement the multi-band system. The first one consists in transmitting all the OFDM waves at the same time, using only one shoot; while in the second approach each OFDM signal is transmitted in a sequential mode [33] [34]. The second option is the simplest one for processing and analysis, so it is adopted in this work for the reconstruction of multi-layer soil permittivity. As an example, the spectrum of the a multi-band OFDM signal with M=5 carriers (0.3GHz, 1.3GHz, 2.3GHz, 3.3GHz, 4.3GHz) is illustrated in figure 2.8.

2.5 Algorithm for the Soil Dielectric Characterization

In this section the algorithm, based on the OFDM multi-band radar signal processing, for the soil's discontinuities detection is presented. A soil can be composed of several layers, each with a different dielectric constant. To test

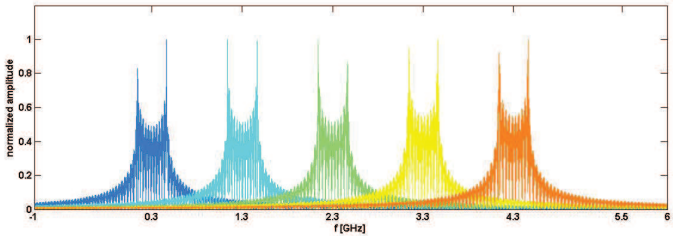

Fig. 2.8. Spectrum of OFDM multi-band signal with M=5 carriers

the algorithm a simple soil structure with two layers, having a thickness d_1 and d_2 and dielectric constant ϵ_1 and ϵ_2 respectively, has been considered (fig. 2.9). A radar signal from a distance $d_0 > \dfrac{2D^2}{\lambda_{min}}$ is assumed to impinge

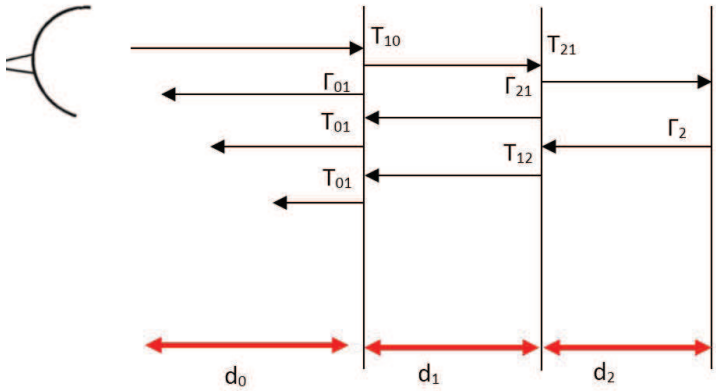

Fig. 2.9. Multi layer test structure.

orthogonally the soil structure; where D is the maximum size of the radar antenna and λ_{min} is the wavelength related to the minimum frequency f_{min} used in the analysis. This condition ensures that the signal is a wave plane form. To obtain the permittivity values of the two layers an OFDM signal single band is considered. The corresponding signal received from the RX antenna can be expressed as:

$$rx(t) = b_0 g(t-\tau_0)e^{j2\pi f_0(t-\tau_0)} + b_1 g(t-\tau_1)e^{j2\pi f_0(t-\tau_1)} + b_2 g(t-\tau_2)e^{j2\pi f_0(t-\tau_2)} \tag{2.22}$$

where:

- b_0 is related to the reflection coefficient Γ_{01} of the first interface and τ_0 is the associated delay;
- b_1 is related to the expression $(1-\Gamma_{01}^2)\Gamma_{12}$ of the second interface and τ_1 is the associated time delay;
- b_2 is related to the expression $(1-\Gamma_{12}^2)\Gamma_{23}$ if the third interface and τ_2 is the associated delay time.

The terms $\Gamma_{01}, \Gamma_{12}$and Γ_{23} are the reflection coefficients at each interface and well known in literature [35].

Before starting the analysis a preliminary calibration must be performed, placing a perfect conductor that covers the test structure as depicted in figure 2.10

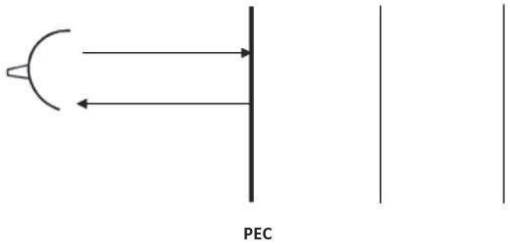

Fig. 2.10. Test structure during the calibration.

The result of the OFDM radar processing is shown in figure 2.11 where the three peaks, corresponding to the reflections due to the three interfaces, together at the peak due to the calibration can be observed. The value obtained from the calibration with the PEC is used as a reference for the algorithm.

A recursive process is applied to obtain the dielectric constant ϵ_{r1} and ϵ_{r2} of the layers, so starting from:

$$b_0 = \Gamma_{01} = \frac{1-\sqrt{\epsilon_{r1}}}{1+\sqrt{\epsilon_{r1}}} \tag{2.23}$$

the value of ϵ_{r1} is straightforwardly retrieved

$$\epsilon_{r1} = \left(\frac{1-\Gamma_{01}}{1+\Gamma_{01}}\right)^2 \tag{2.24}$$

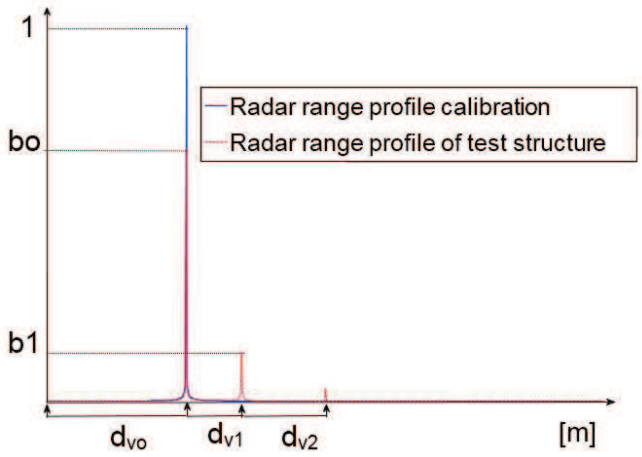

Fig. 2.11. Radar range profile.

So, we can use the following steps to retrieve the value of $\sqrt{\epsilon_{r2}}$ and repeat them for the successive substrate.

$$\frac{b_1}{b_0} = \frac{(1-\Gamma_{01}^2)}{\Gamma_{01}}\Gamma_{12} \tag{2.25}$$

from equation 2.25 Γ_{12} can be obtained and subsequently the value of ϵ_{r2}:

$$\Gamma_{12} = \frac{\sqrt{\epsilon_{r2}} - \sqrt{\epsilon_{r1}}}{\sqrt{\epsilon_{r2}} + \sqrt{\epsilon_{r1}}} \tag{2.26}$$

$$\epsilon_{r2} = \left(\frac{1+\Gamma_{12}}{1-\Gamma_{12}}\sqrt{\epsilon_{r1}}\right)^2 \tag{2.27}$$

where ϵ_{r1} was computed in the previous iteration.

A generalized form of the equations for the algorithm can be expressed as:

$$\frac{b_n}{b_{n-1}} = \frac{(1-\Gamma_{n-1,n}^2)}{\Gamma_{n-1,n}}\Gamma_{n,n+1} \tag{2.28}$$

$$\epsilon_{r,n} = \left(\frac{1+\Gamma_{n-1,n}}{1-\Gamma_{n-1,n}}\sqrt{\epsilon_{r,n-1}}\right)^2 \tag{2.29}$$

where the term n indicates the n^{th} discontinuities.

Once the dielectric constant of the layers is computed, the next step is that of computing the real thickness of the substrates.

$$d_i = \frac{d_{vi}}{\sqrt{\epsilon_{ri}}} \tag{2.30}$$

Let us assume, now, that the layers in figure 2.9 are composed by dispersive media, with a variation of permittivity versus frequency. In this case, a multi-band OFDM technique can be adopted to retrieve the variation profile of dielectric constants. In particular, by considering M different carriers as in figure 2.8, the algorithm, previously described for the case of single band OFDM, must be repeated for every carrier frequency, thus obtaining M graphs similar to that of figure 2.11, but with a shift Δd, variable versus frequency, for the distances d_{v1} and d_{v2}. This shift Δd is related to the permittivity shift $\Delta\epsilon_r$, which can be expressed as:

$$\Delta\epsilon_r = \left(\frac{d_{vi}}{d_{vi} - \Delta_d}\right)^2 \tag{2.31}$$

2.6 Numerical Results

In order to validate the proposed multi-band algorithm, the multi-layer soil structure in figure 2.12 is assumed as test scenario. The values of dielectric constant for the two layers under analysis was obtained using the empirical models discussed in section 2.3. In particular, the input of the models are in terms of clay percentage C, sand percentage S and the water content θ as reported in table 2.1, where the respectively retrieved dielectric constant is also indicated.

As a first task, a single-band OFDM radar signal with $f_0 = 2.3GHz$ is assumed to retrieve the the value of ϵ_{r1} and ϵ_{r2} and the thickness d_1 and d_2 of the two layers, according to the equation 2.26 and 2.27. The preliminary calibration phase using a perfect conductor (PEC) has been considered during the validation test.

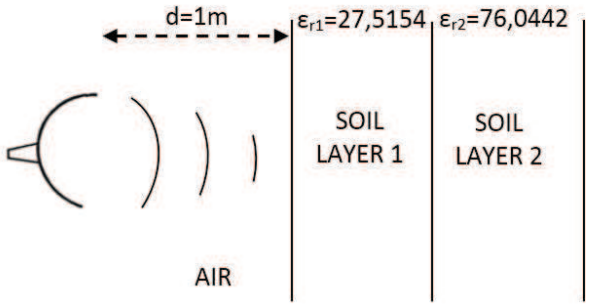

Fig. 2.12. Simulated Scenario.

Table 2.1. Input of the soil electrical model.

	Soil Layer 1	Soil Layer 2
θ	0.27	0.8
S	0.95	0.70
C	0.02	0.01
ϵ_r	27.5154	76.0442

Subsequently, the multi-band OFDM signal with M = 3 carriers from 2.3 GHz up to 4.3 GHz is considered. The relative detected values of Δd, variable with carrier frequency are then used to obtain the variation profile of the permittivity as a function of frequency, for the two soil layers. The results of the numerical analysis and then, the retrieved ϵ_{r1} and ϵ_{r2} and their variation respect to the frequency are reported in table 2.2 and table 2.3

Table 2.2. Retrieved permittivity and thickness

	Soil Layer 1	Soil Layer 2
Retrieved ϵ_r	26.8856	72.1654
Retrieved layer thickness [m]	0.3934	0.4453

In figure 2.13 the results of the OFDM multi-band processing is reported and the shift δd d is evidenced.

Table 2.3. Retrieved permittivity and thickness

f [GHz]	$\Delta\epsilon_{r1}$	$\Delta\epsilon_{r1}$
2.3	1.0314	1.0503
3.3	1.0314	1.0502
4.3	1.0314	1.0726

In the graphs reported in figure 2.14 and 2.15 a comparison between the software retrieved dielectric constant and the one computed by the empirical model have been reported; respectively for the first and second layers.

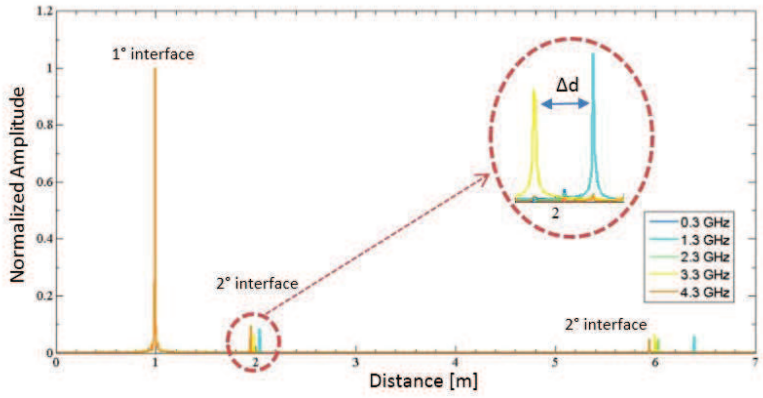

Fig. 2.13. Shift effect on the retrieved signal peaks.

2.7 Conclusion

The adoption of the Software Defined concept to realize measurement systems (SDM) is a new trend in this research field. In this chapter, the combination of the OFDM radar processing with the software defined radar technologies has been discussed, in order to realize a Software Defined Measurement platform for soil electrical properties. The advantageous features of Software Defined Radar technology, in terms of the easy implementation of signal processing algorithms, have been exploited. The demonstration, via numerical simulations, that the Orthogonal Frequency Division Multiplexing processing is well situated to implement a multi-band system, able to accurately retrieve the

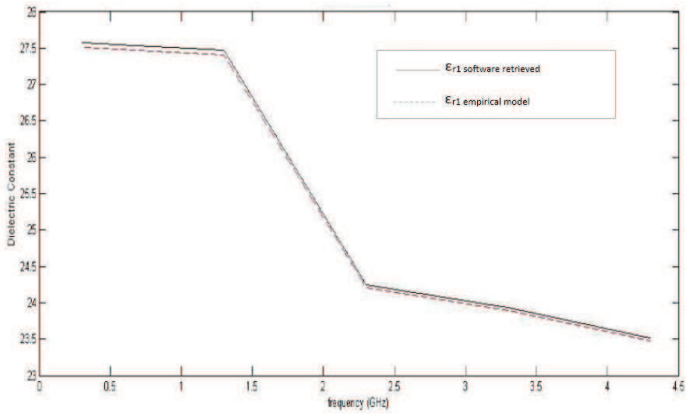

Fig. 2.14. ϵ_{r1} software retrieved and ϵ_{r1}compute by empirical model vs. frequency

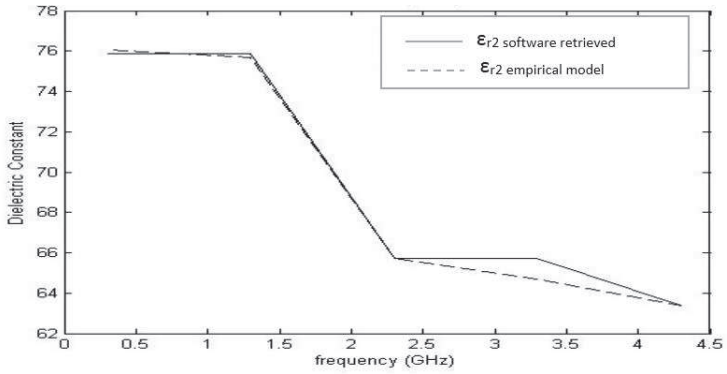

Fig. 2.15. ϵ_{r2} software retrieved and ϵ_{r2}compute by empirical model vs. frequency

geometrical and dielectric profiles of multi-layer soils, and to compute the behaviour of the permittivity versus the frequency has been treated in this work. The new challenge to extend the implemented algorithm to the imaginary part of the dielectric constant is object of future work; for this reason, more accurate models for the multi-layer structure and new and more efficient algorithms for the dielectric characterization will be very soon considered.

3

Next Generation Radar

3.1 Introduction

The Birth of radar dates back to 114 years ago, when the German engineer C. Hulsmeyer patented the Telemobiloscope, a useful device to avoid the collision between the ships in adverse conditions of sailing. In radar development Italy has always played an important role. In 1930,during the testing of transoceanic radio broadcasts, Guglielmo Marconi demonstrated the ability to detect objects using electromagnetic waves. Ugo Tiberio father of Italian radar, following this experience, presented a report to the military authorities, in which the radar equation in free space was, for the first time, obtained.
The standard structure with reflector antennas and mechanical rotation in use until the 80s, was replace by the phased array that allow beam control in elevation and azimuth, in order to obtain adaptively and functionality of radar systems. The use of Doppler frequency opened the way to new performances, such as the detection of moving targets and the estimation of the instantaneous radial velocity until SAR systems. The further evolution provides a fully digital radar, able to implement multifunctional applications into a cognitive system based on software. In this final chapter a brief introduction to the new radar technologies is given emphasizing the importance of the Software Defined Radar.

3.2 The New Radar Technologies

The radio frequency systems have been significantly improved creating many new challenges in the research of radar system. Future Radars must be ex-

pressively enhanced in their radio frequency system concepts to meet the requirements for angular, range and Doppler information; simultaneous wide area coverage but still high angular resolution; low interference with other RF systems; for digital processing for all dimensions, smaller hardware and, last but not least, they must become cheaper. Compared to several decades ago, Radar applications have now spread to many new areas: automotive radars, surveillance, medical applications, imaging, remote sensing and so on. Some of these applications are expected in numbers of millions in the future.

The author in [28] introduces the future radar systems by claiming that radio frequency design has not changed accordingly with the advanced state of art of other areas in communication engineering. The consequence is that the time is pressing for the integration of new ideas for radar system concept. The intelligent Signal Coding, MIMO radar, Digital Beam forming, Array Imaging and Compressive sensing belong to the present radar state of art. These concepts introduce the possibilities to realize a RadCom [36], a device able to do radar detection and communication. In addition to these Cognitive Radar systems are defined the last trend in radar technologies. **Software Defined Radar Systems** are the fundamental of all these new technologies.

RadCom Systems.
The most useful signals in radar application are chirp signal and pulse signal; generally pulsed radar are used for far range application, while FM-CW radar based on chirp signal are mostly used for near range applications, but in some cases there are exceptions. These two kinds of signal do not transport any information they are simple radar signals. One of the main idea in radar field is the use of intelligent signal coding to do radar detection and at the same time a communication system in order to create a **RadCom**.
The main challenge in establishing a RadCom system is to identify a suitable waveform for both the joint operations. In [36] [37] the authors discuss the OFDM signals, which are suitable for both radar and communications; in particular, OFDM signal offers the best feature for intelligent radar usage. The idea of combining communication and radar first came up during the developments triggered by the Second World War. However, active development on combined systems is rare. One of the few examples of deployed combined systems was implemented in the NASA Space Shuttle Orbiter. This system could switch between radar and communications functionality, but not per-

form both at the same time. A RadCom system finds application in several areas; in particular, in vehicular ad hoc networks *VANET*, where a car-to-car communication has been performed to prevent the accident situation (figure 3.1) [24].

Software defined radar sensor, where the entire signal processing can be modified via software, could be an ideal candidate for implementing a combined radar and communication device. The author in [10] presents a measurement testbed for OFDM radar, in which the USRP platform is used as a front-end to implement both Radar and Communication Systems. In this paper, the proof that the Software Defined platform USRP, widely treated in this thesis, is very suitable for radar and RadCom application.

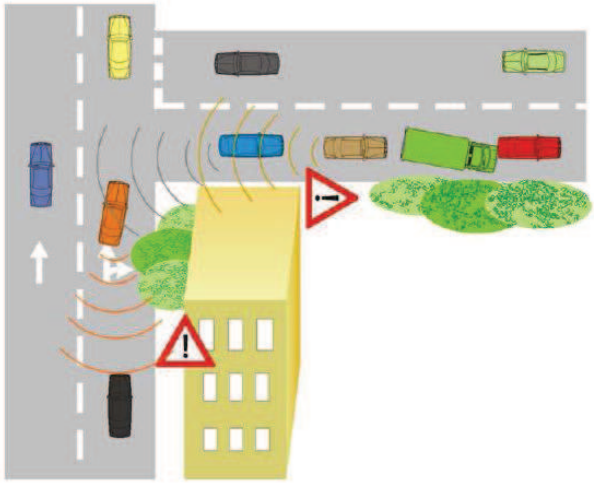

Fig. 3.1. A traffic situation: Car use their sensor to detect an accident and transmit this information to other vehicles which might not have line of sight to the danger.

MIMO Radar

It has been recently shown that multiple-input multiple-output (MIMO) antenna systems have the potential to dramatically improve the performance of communication systems over single antenna systems. The improvement is mainly in terms of signal to noise ratio and multipath-fading. Recently this concept has been spread to radar system [38]. The notion of MIMO radar is simply that there are multiple radiating and receiving antennas. The basic idea

is to transmit (and receive) identical information via multiple antennas with different codes over different or identical propagation paths. In order to make this possible the multiple transmit signals have to be highly de-correlated. In much of the current literature, it is assumed that the waveforms coming from each transmit antenna are orthogonal, but this is not a requirement for MIMO radar [39].
Like MIMO communications, MIMO radar offers a new paradigm for signal processing research. MIMO radar possesses significant potentials for fading mitigation, resolution enhancement, and interference and jamming suppression; fully exploiting these potentials can result in much improved target detection and recognition performance [40]. The main difference with the classical radar systems, like a phased array radar, is in the illumination pattern (figure 3.2); in a radar using phased array antenna a single waveform shifted in phase is transmitted, while in MIMO radar systems multiple differential waveforms are used. This feature improves the maximum number of detectable targets.

Generally there are two ways of using of MIMO radar [39]. The first one is called *statistical MIMO radar* where both transmit and receive array elements are largely spaced in order to perform independent scattering response for each TX RX antenna. The second configuration is defined *coherent MIMO radar*; in this case the transmit array elements (and receive array elements) are closely spaced. This configuration allows the same scattering response for each antenna pair with the exception of some delays determining azimuth resolution improvement. In some sense, the performance of the MIMO systems can be characterized by the position of the transmit and receive array elements.
The waveform diversity enables superior capabilities compared with a standard phased-array radar; in particular the *parameter identifiability*, which is the maximum number of targets that can be uniquely identified by the radar, is highly improved compared to the radar based on the classical phased-array [41].

The author in [28] suggests the use of intelligent signal coding in MIMO radar in order to facilitate the de-correlation of the transmitted signal; the author underlines the use of the OFDM signal coding in order to retain the total signal bandwidth and to ensure a high SNR level and de-correlation.

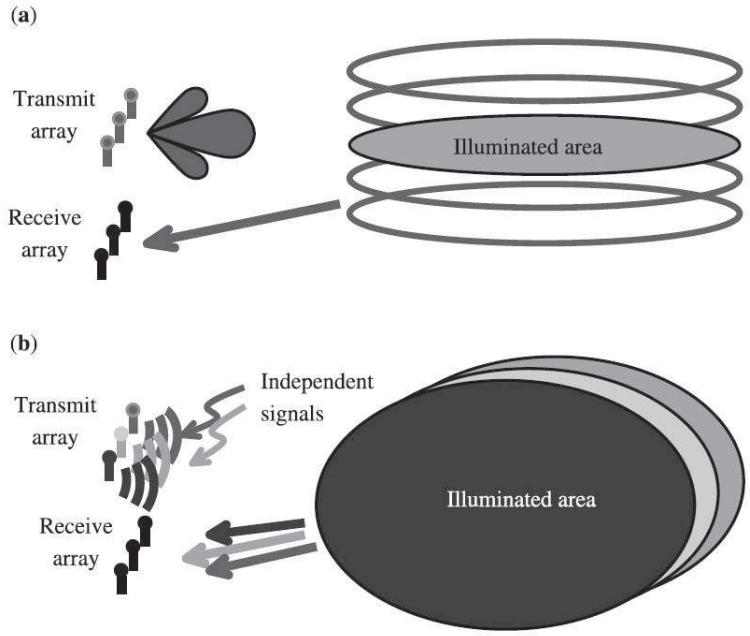

Fig. 3.2. (a) Classical radar scenario, (b) Mimo radar scenario

Digital Beamforming

A new area in radar and radio research, which has the software defined system as a basis principle, is the Digital Beamforming. Beamforming is the combination of radio signals from a set of small non-directional antennas to simulate a large directional antenna; specifically, it is a powerful technique to enhance antenna performance. The simulated antenna can be pointed electronically, although the antenna does not physically move; practically DBF is a new feeding technique of the antenna.

In communications, beamforming technique is used to point an antenna to reduce interference and improve communication quality. In direction finding applications, beamforming can be used to steer an antenna to determine the direction of the signal source [42]. The basic idea is that the received signals of each RX antenna are separately amplified, down-converted and digitized [43]; this allows the use of small and fixed antennas to illuminate a wide swath on the ground. A block diagram of the receiver system is reported in figure 3.3. The main advantages of DBF are realized in the receive mode: improved

adaptive pattern nulling; closely spaced multiple beams; array element pattern correction; antenna self-calibration and ultralow sidelobes; super-resolution; and flexible radar power and time management [44].

In radar research a DBF antenna system is used to improve the azimuth resolution through a virtual receive beam, in order to see small objects surrounded by clutter, for example, in military application, the detection of a Drone is more difficult than that of a Boeing.

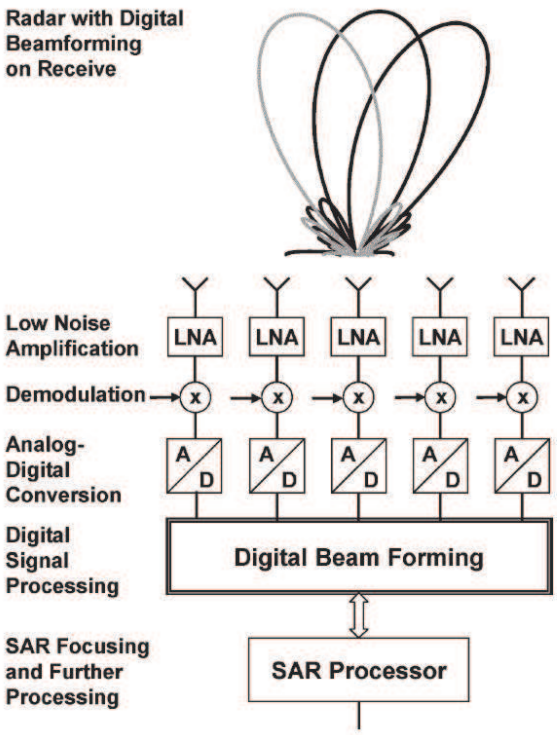

Fig. 3.3. Block Diagram of a radar receiver based on Digital Beamforming.

Digital Beamforming antenna is quite different from a mechanical rotating-antenna radar or from the conventional phased array radar in which it can carry out multiple functions simultaneously rather than sequentially.
Thus it has the important advantage that its various functions do not have to be performed in sequence one at a time, which is a serious limitation of

conventional phased arrays. The DBF antenna is a new method to achieve important radar capabilities, not available with current radar architectures, especially in SAR systems where wide swath coverage and high azimuth resolution create several limitation. Other advantages are the good signal to noise ratio; the disposal of mechanical rotation like in classical radar; the loss reduction due to the disposal of additional network for beam steering, but now they do not have reasonable costs.

Compressive Sensing

In several radar application an appropriate radar slant range resolution is required, so the principal challenge in radar field is the improvement of this parameter, in order to obtain more and more precisely image reconstruction. The main radar formula expressing the range resolution is $\Delta_r = \frac{c}{2B}$ where B is the radar signal bandwidth and c is the speed of the light. For example a radar system that requires a $\Delta_r = 5mm$, a bandwidth equal 150GHz is necessary. To convert a radar signal correctly from analogue to digital domain, following the Nyquist-Shannons theorem, the sampling rate must be at least twice the bandwidth. This is impossible to meet with the current technologies.

In the radar and communication state of art, the concept of Compressive Sensing/Sampling (CS) is defined as a new paradigm that goes against the common knowledge in data acquisition [45].

The compressive Sampling theory asserts the possibility to reconstruct certain signal from a few samples, in disagreement with the traditional sampling theory.

Compressive sensing techniques generally deal with incomplete linear equation systems of the type $y = Ax$

There is a variety of algorithms aiming to reconstruct x from the deterministic measurements $y = Ax$ or the noisy measurements $y = Ax + n$ under the assumption that x is sparse.

The most elementary task in radar field is pulse compression, treated in a large number of papers, where sparse sampling can be applied in the fast time domain as well as in the frequency domain . For example in [46] the improvement of radar slant range resolution of Stepped Frequency Continuous Wave (SFCW) Radar is discussed.

In [47] Compressive Sensing is applied to MIMO radar, the paper presents a CS stepped frequency MIMO radar in order to the provide high resolution range, angle and Doppler estimation. In applications like Synthetic Aperture Radar (SAR) where the image information is only in the two native coordinates azimuth and range, the compressive sensing is a great solution for the retrieving of the third dimension, the elevation angle [48]. The Compressive Sensing applied to radar task opens a new view to radar sensing and shows new possibilities chancing the classical signal processing approach; nevertheless, Compressive Sensing technique needs more detailed study in order to judge objectively the profit against classical methods. Recently Compressive sensing is also applied in array diagnosis [49]

Cognitive Radar

The Software Defined Systems have widely improved the research on Information and Communication Technologies.

As the Software Defined Radio system provides the basis for the new area of research, Cognitive Radio [50], so from SDRadar systems the Cognitive Radar system starts. This kind of radar reach high levels of importance in radar research, so it is only right to make a lightweight description of its operation mode and state of art.

The Cognitive Radar concept and term was first introduced by Simon Haykin in 2006 in a Special Issue of IEEE Signal Processing Magazine on Knowledge-Based Systems for Adaptive Radar [51]. According to Haykin there are three ingredients that are basic to the constitution of a cognitive radar:

1. intelligent signal processing, which builds on learning through interactions of the radar with the surrounding environment;
2. feedback from the receiver to the transmitter, which is a facilitator of intelligence;
3. preservation of the information content of radar returns, which is realized by a Bayesian approach to target detection through tracking.

In [52] the author expands the idea of cognitive radar underlying that the cognition is the key for the next generation radar. In [53] a simulated closed-loop of a active radar sensor by updating the probabilities on an ensemble of target hypotheses in order to analyse the performance of a cognitive sensor is presented. Furthermore, the problem of waveform selection for cognitive

system is widely treated in literature, [54] [55], while the combination of the OFDM radar processing in a Cognitive system is dealt in [56].

A good description of the operation mode of a Cognitive Radar system is given in [57]. In table 3.1 is shown a correspondence between the term "*cognitive*" and the function of a radar systems.

Table 3.1. Mapping of biological cognitive properties to that a cognitive radar

Cognitive Property	**Cognitive Radar equivalent**
Perceiving	Sensing
Thinking	Expert system, Adaptive algorithm and computation
Remembering	Memory, Enviromental Database

The architecture of a Cognitive Radar,as shown in figure 3.4, is characterized by the introduction of a dynamic environmental database (EDDB), by a feedback between the transmitter and the receiver and by an adaptive transmitter and receiver.

Fig. 3.4. Cognitive Radar Architecture.

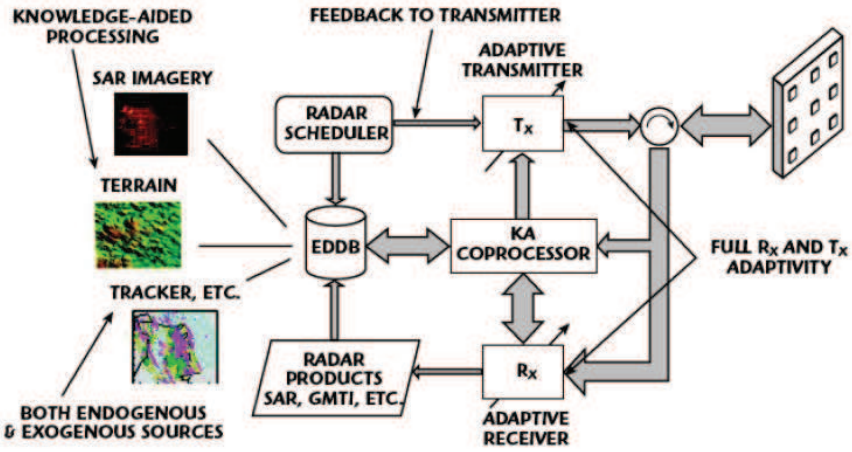

The information received by the RX antenna is stored in the EBBD in order to create a knowledge base of the environmental in which the radar system is applied. The same information is processed and each time passed

to the transmitter which adapts its waveform in order to increase the entire performance of the system. So there two main concepts in a Cognitive Radar System: *diversity in transmission* and *processing aided by knowledge* The architecture in figure 3.4 is able to implement an adaptivity on different scenarios by simulating a biological cognitive system.

4

Conclusion

In this thesis, the potentialities and benefits of Software Defined Radar system have been investigated. The striking difference between traditional and software radar systems is in the use of software and programmable logic modules to replace components typically implemented using dedicated hardware, such as demodulators filters and mixers.
This new technology offers an high degree of adaptability and flexibility in the design of new prototypes of radar; among the main advantages, the multipurpose features will provide the possibility to implements several kind of radar with several task in the same hardware.
Then, the Software Defined Radar has been considered an excellent solution to overcome the limitation imposed by the hardware for some years. Furthermore, these systems opened the doors to the studies on other branches related to radar that certainly improve the quality of life and the quality of the future research. The main examples of this are the Digital Beam-forming and the Cognitive Radar system.
In order to prove all these features, this thesis focused the attention, in the first chapter, on the developed of an L-band SDRadar system based on the use of the hardware platform USRP NI 2920.

The Universal Software Radio Peripheral is a flexible software defined transceiver born for didactic purposes, and the characterization in radar field of this board has been the focus of the entire work during these 3 years of PhD course. First of all a detailed analysis of the USRP NI2920 operation mode has been performed identifying the key features in terms of radar. A comparison between the new and the old version of USRP has been carried out, providing,

as a result, a strong improvement in the radar slant range resolution, more precisely $\Delta R = 6m$ for the USRP NI 2920 and $\Delta R = 37.5m$ for the first generation USRP. This means that USRP NI 2920 can be applied in several radar applications. The implementation of the L-band SDRadar with a complete mechanical scanning system and remote control has been performed. In order to validate the system designed, indoor and outdoor experimental tests have been carried out with optimum results; in particular, during the tests the capacity of the foliage penetration using the L-band has been verified.
Furthermore, an application of software defined measurement system for the detection of soil electrical properties has been discussed. In this part a multiband OFDM radar system has been proposed as a signal processing technique of an novel algorithm for soil discontinuity detections. In order to verify the correctness of the algorithm proposed, the numerical results have been compared with two empirical models for the soil dielectric properties, widely treated in scientific literature.
The SDRadar system developed during the Ph.D will be applied in the framework of the National Project *"LANDSLIDE AND EARLYWARNING"* to monitor a landslide situated above a national highway. The future tests will be certainly useful to understand the critical points in the landslide monitoring.

References

1. Wiesbeck Werner. SDRS: software-defined radar sensors. In: Geoscience and Remote Sensing Symposium, 2001. IGARSS'01. IEEE 2001 International. IEEE, 2001. p. 3259-3261.
2. Lee K Patton . A GNU radio based software-defined radar. Diss. Wright State University, 2007.
3. T. Debatty, Software defined RADAR a state of the art, 2010 2nd International Workshop on Cognitive Information Processing, Elba Island, Italy: 2010, pagg. 253- 257.
4. Ettus, M., USRP user's and develeper's guide," Aug. 2006, http://www.ettus.com/.
5. Zhang, Hui, Lin Li, and Ke Wu. "24GHz software-defined radar system for automotive applications." Wireless Technologies, 2007 European Conference on. IEEE, 2007.
6. Braun, Martin, et al. "Parametrization of joint-based radar and communication systems for vehicular applications." Personal, Indoor and Mobile Radio Communications, 2009 IEEE 20th International Symposium on. IEEE, 2009.
7. Capria A. et al. "Ship detection with DVB-T software defined passive radar." IEEE Gold Remote Sensing Conference. 2010.
8. Chinnam, Deepthi Maheswari, et al. "Implementation of a low cost synthetic aperture radar using software defined radio." Computing Communication and Networking Technologies (ICCCNT), 2010 International Conference on. IEEE, 2010.
9. Fernandes V.N. Implementation of a RADAR System using MATLAB and the USRP. 2012. PhD Thesis. California State University, Northridge.
10. Braun, Martin, et al. "A USRP-based Testbed for OFDM-based Radar and Communication Systems." Proceedings of 22nd Virginia Tech. Symposium on Wireless Communications. 2012.

11. Capria, Amerigo, et al. "Ship detection with DVB-T software defined passive radar." IEEE Gold Remote Sensing Conference. 2010.
12. S. Costanzo, F. Spadafora, G. Di Massa, A. Borgia, A. Costanzo, G. Aloi, P. Pace, V. Loscri, and H. O. Moreno: Potentialities Of Usrp-Based Software Defined Radar Systems: Progress In Electromagnetics Research B (Pier B) vol. 53, 2013
13. S. Costanzo, F. Spadafora, A. Borgia, H. Moreno, A. Costanzo, G. Di Massa: High Resolution Software Defined Radar System for Target Detection, Advances in Intelligent Systems and Computing Volume 206, 2013, pp 997-1005
14. Ettus Research, USRP bandwidth on http://www.ettus.com/kb/detail/usrp-bandwidth
15. G.Aloi, A. Borgia, S.Costanzo, G. Di Massa,V. Loscr,E. Natalizio, P.Pace, F Spadafora "Software defined radar: synchronization issues and practical implementation." Proceedings of the 4th International Conference on Cognitive Radio and Advanced Spectrum Management. ACM, 2011.
16. Mahafza, B. R. and A. Z. Elsherbeni, Simulations for Radar Systems Design, CHAPMAN and HALL/CRC, 2003.
17. DAVIS M. Foliage penetration radar. The Institution of Engineering and Technology, 2011.
18. Costanzo S., Di Massa G.,Costanzo A., Borgia A., Papa C., Alberti G., Salzillo G., Palmese G., Califano D., Ciofanello L., Daniele M., Facchinetti C., Longo F., and Formaro R., Multimode/Multifrequency Low Frequency Airborne Radar Design,Journal of Electrical and Computer Engineering, 2013.
19. Mahafza, B. R. and A. Z. Elsherbeni, Simulations for Radar Systems Design, CHAPMAN and HALL/CRC, 2003.
20. S.Costanzo,G.Di Massa,D.Moreno, F. Spadafora, Multipurpose Software Defined Measurement system for dielectric characterization. In: Antennas and Propagation (EuCAP), 2014 8th European Conference on. IEEE, 2014. p. 1090-1091.
21. S. Costanzo, I.Venneri, G. DI Massa, A.Borgia, Benzocyclobutene as substrate material for planar millimeter-wave structures: dielectric characterization and application. Journal of Infrared, Millimeter, and Terahertz Waves, 2010, 31.1: 66-77
22. J. Baker-Jarvis, et al. Dielectric characterization of low-loss materials a comparison of techniques. IEEE Transactions on Dielectric and Electrical Insulation, 1998, 5.4.
23. G.Di Massa, S.Costanzo,O.H. Moreno, Accurate circuit model of open resonator system for dielectric material characterization. Journal of Electromagnetic Waves and Applications, 2012, 26.5-6: 783-794.

24. M.Braun, OFDM Radar Algorithms in Mobile Communication Networks. 2014. PhD Thesis. Karlsruhe, Karlsruher Institut fur Technologie (KIT), Diss., 2014.
25. Neil R. Peplinski, Fawwaz T. Ulaby, and Myron C. Dobson, Dielectric Properties of soil in the 0.3-1.3-Ghz Range, IEEE Trancactions on Geoscience and Remote Sensing, Vol. 33, No. 3, May 1995.
26. Timothy W.Miller, Brian Borchers, Jan M.H. Hendrickx, Sung-Ho Hong, Louis W. Dekker, and Coen J. Ritsema, Effects of soil physical properties on GPR for landmine detection, Fifth International Symposium on Technology and the Mine Problem, 2002.
27. M. C. Dobson, F. T. Ulaby, M. T. Hallikainen, and M. A. El-Rayes, Microwave dielectric behavior of wet soil - Part II: Dielectric mixing models, IEEE Trans. Geosci. Remote Sens., 23, pp. 35-46, 1985.E
28. W.Wiesbeck, The Radar of the Future,Proceedings of the 10th European Radar Conference, Nuremberg,2013.
29. Christian Sturm, Thomas Zwick, and Werner Wiesbeck, An OFDM System Concept for Joint Radar and Communications Operations, Institut fr Hochfrequenztechnik und Elektronik, University of Karlsruhe (TH) Kaiserstrae 12, 76131 Karlsruhe, Germany, 978-1-4244-2517-4/09, 2009 IEEE;
30. Martin Braun, Christian Sturm and Friedrich K. Jondral, Maximum Likelihood Speed and Distance Estimation for OFDM Radar, Communications Engineering Lab, Karlsruhe Institute of Technology (KIT), Germany, Institut fur Hochfrequenztechnik und Elektronik, Karlsruhe Institute of Technology (KIT), Germany, 2010;
31. Manuel Fuhr, Martin Braun, Christian Sturm, Lars Reichardt and Friedrich K. Jondral, An SDR-based Experimental Setup for OFDM-based Radar, Communications Engineering Lab, Karlsruhe Institute of Technology (KIT), Germany zInstitut fur Hochfrequenztechnik und Elektronik, Karlsruhe Institute of Technology (KIT), Germany;
32. Martin Braun, Thomas Schu, Christian Sturm and Friedrich K. Jondral, On the Single-Target Accuracy of OFDM Radar Algorithms, Communications Engineering Lab, Karlsruhe Institute of Technology (KIT), Germany Institut fur Hochfrequenztechnik und Elektronik, Karlsruhe Institute of Technology (KIT), Germany, 2011;
33. S.Costanzo, F.Spadafora, H.O. Moreno F. Scarcella, G.Di Massa, Muli-Band Software Defined Radar for soil discontinuities detection,Journal of Electrical and Computer Engineering, 2013, 2013: 5.
34. S.Costanzo, G.Di Massa, D. Moreno, F.Spadafora, Multipurpose Software Defined Measurement system for dielectric characterization. In: Antennas and Propagation (EuCAP), 2014 8th European Conference on. IEEE, 2014. p. 1090-1091

35. C. A. Balanis, Advanced Engineering Electromagnetic, John Wiley and Sons, 1989
36. Braun M., Sturm C. , Jondral, F. K, On the Frame Design for Joint OFDM Radar and Communications. In: 15th International OFDM Workshop, Hamburg. 2010.
37. A.Suban, G.Thanga Balaji, H.Mani Aravinth and C.Kaleeswaran,OFDM Based Radcom System with Improved Performance Using Digital Beamforming Technique,International Journal of Computational Science and Information Technology (IJCSITY) Vol.2, No.2, May 2014
38. FISHLER E., et al. MIMO radar: an idea whose time has come. In: Radar Conference, 2004. Proceedings of the IEEE. IEEE, 2004. p. 71-78.
39. Li, Jian, and Petre Stoica, MIMO radar signal processing. Hoboken, NJ: J. Wiley and Sons, 2009.
40. LI, Jian, et al. Introduction to the issue on MIMO radar and its applications. Selected Topics in Signal Processing, IEEE Journal of, 2010, 4.1: 2-4.
41. L. Jian; S. Petre. MIMO radardiversity means superiority. In: Proceedings of the 14th adaptive sensor array processing workshop (ASAP06). 2009. p. 1-6.
42. Haynes T. A primer on digital beamforming. Spectrum Signal Processing 11 (1998).
43. G. KKrieger ,N. Gebert, A. Moreira, Multidimensional waveform encoding: A new digital beamforming technique for synthetic aperture radar remote sensing. Geoscience and Remote Sensing, IEEE Transactions on, 2008, 46.1: 31-46
44. H. Steyskal, Digital beamforming antennas-An introduction. Microwave Journal, 1987, 30: 107.
45. E. J. Cands, M. B. Wakin, An introduction to compressive sampling. Signal Processing Magazine, IEEE, 2008, 25.2: 21-30
46. I. Sarkas, Step Frequency Radar Using Compressed Sensing,Department of Mathematics of the University of Toronto, Tech. Rep, 2010.
47. Y.YYu, A. P. Petropulu, H. V. Poor, CSSF MIMO radar: Low-complexity compressive sensing based MIMO radar that uses step frequency. *arXiv preprint* arXiv:1101.2719, 2011.
48. Z.X. Xiang, R. Bamler.. Demonstration of super-resolution for tomographic SAR imaging in urban environment. Geoscience and Remote Sensing, IEEE Transactions on, 2012, 50.8: 3150-3157.
49. S. Costanzo, A. Borgia, G. Di Massa, D. Pinchera, M. D. Migliore, Radar array diagnosis from undersampled data using a compressed sensing/sparse recovery technique. Journal of Electrical and Computer Engineering, 2013.
50. J. MITOLA, Cognitive Radio—An Integrated Agent Architecture for Software Defined Radio. 2000.

51. S.Haykin, Cognitive radar in IEEE Signal Processing Magazine, Vol 30 January 2006, pp. 30-40.
52. S. Haykin, Cognition is the key to the next generation of radar systems, Digital Signal Processing Workshop and 5th IEEE Signal Processing Education Workshop, 2009. DSP/SPE 2009. IEEE 13th, pp. 463-467.
53. Nathan A. Goodman, Phaneendra R. Venkata and Mark A. Neifeld, Adaptive waveform design and sequential hypothesis testing for target recognition with active sensors, IEEE Journal of Selected Topics in Signal Processing, 2007, 1(1), pp. 105-113.
54. Y. He and E. K. P. Chong, Sensor scheduling for target tracking in sensor networks, 43rd IEEE Conference on Decision and Control, Paradise, Island, Bahamas, 2004, pp. 743-748.
55. V.Krishnamurthy, Algorithms for optimal scheduling of hidden Markov model sensors, IEEE Trans. on Signal Processing, 2002, 50(6), pp.1382-1397.
56. B.Jameson, D. Garmatyuk, J. Morton. Cognitive radar for indoor positioning with a software-defined UWB OFDM system. Radar Conference (RADAR), 2012 IEEE. IEEE, 2012.
57. Guerci, Joseph R. "Cognitive radar: a knowledge-aided fully adaptive approach." Radar Conference, 2010 IEEE. IEEE, 2010.